An insight into an autophagy receptor p62 oligomerization through PB1 domain using molecular modeling

by

Nan Wu

Bachelor's degree, China Pharmaceutical University, 2017

Submitted to the Graduate Faculty of

School of Pharmacy in partial fulfillment

of the requirements for the degree of

Master of Science

University of Pittsburgh

2019

UNIVERSITY OF PITTSBURGH

SCHOOL OF PHARMACY

This thesis was presented

by

Nan Wu

2

It was defended on

March 18th, 2019

and approved by

Levent Kirisci, PhD, Professor, Department of Pharmaceutical Science

Xiang-Qun (Sean) Xie, PhD, EMBA, Professor, Department of Pharmaceutical Science

Zhiwei Feng, PhD, Assistant Professor, Department of Pharmaceutical Science

Jaden Jungho Jun, PhD, Assistant Professor, Department of Pharmaceutical Science

Thesis Director: Xiang-Qun (Sean) Xie, PhD, MD, EMBA, Department of Pharmaceutical Science

An insight into an autophagy receptor p62 oligomerization through PB1 domain using molecular modeling

Nan Wu, BS

University of Pittsburgh, 2019

ABSTRACT

Autophagy is a term of the ancient process in eukaryotic cells, which is responsible for transporting and degrading the 'bad proteins' to promote the cell survival. The Nobel Assembly at Karolinska Institute awarded the 2016 Nobel Prize in Physiology or Medicine to Yoshinori Ohsumi for his discoveries of mechanisms for autophagy. Autophagy has been reported to be related to the regulation of cancer and the neurodegenerative diseases. p62/sequestosome1 (SQSTM1), an autophagy inducer brought about innovative ideas about the treatment of those diseases. p62 is a multi-domain protein and each of its domain will have interactions with partners that are involved in the different physiological processes. Our lab is the first one to build the 3D structure of full-length p62 and has designed compounds (XIE2008 and XIE62-1004) as p62 regulator with experiments published in *Nature Communications*. In this thesis, to address three questions: 1) How p62 PB1-p62 PB1 oligomerized? 2) How newer p62-ZZ compound affect p62 oligomerization? 3) What is the role of second-generation p62-ZZ compound(s) for this process? Firstly, the author briefly discussed the relationship among autophagy, p62 and different kinds of diseases such as Alzheimer's disease (AD), in Parkinson's disease (PD) and Huntington's disease

(HD). Secondly, the author validated published 3D model of full-length of p62 via docking with its partners separately. Importantly, one of p62 domains called PB1 does self-oligomerization and innovative prediction study of the binding conformations between two p62s using Z-DOCK, a rigid-body docking program is discussed. The author constructed p62 PB1-p62 PB1 oligomerization through protein-protein docking and selected the most possible conformation of p62 PB1-p62 PB1 oligomerization. The author selected the most important interacted residues for bio-assay validation.

Keywords: Computer-aided Drug Design (CADD), Docking, Autophagy, p62, PB1-PB1 oligomerization, Neurodegenerative disorders

TABLE OF CONTENTS

PREFACE **12**

1.0 INTRODUCTION **14**

1.1 p62: AN INDUCER OF AUTOPHAGY **14**

1.2 FUNCTIONAL DOMAINS OF p62 ..... **20**

1.3 p62 IN NEUROGENERATIVE DISEASES **24**

1.3.1 REGULATION OF p62 IN PARKINSON'S DISEASE (PD) **24**

1.3.2 REGULATION OF p62 IN HUNTINGTON'S DISEASE (HD) **26**

1.3.3 REGULATION OF p62 IN ALZHEIMER'S DISEASE (AD) **27**

2.0 MATERIALS AND METHODS **29**

2.1 PREPARED DOMAINS **29**

2.2 HOMOLOGY MODEL **30**

2.3 DOCKING **33**

2.3.1 SYBYL DOCKING **33**

2.3.2 Z-DOCK **35**

2.4 MOLECULAR DYNAMICS SIMULATION **39**

3.0 RESULTS **41**

3.1 FULL-LENGTH p62 3D STRUCTURE **41**

3.2 BINDING OF p62 WITH LC3 ..... **43**

3.3 BINDING OF p62 WITH UBIQUITIN **46**

3.4 BINDING OF p62 WITH PKCζ **50**

3.5 BINDING OF p62 WITH RIP1 54

3.6 p62 SELF-OLIGOMERIZATION THROUGH PB1 DOMAIN..... 59

3.7 DYNAMICAL CROSS-CORRELATIONS BETWEEN p62 PB1 AND ZZ DOMAIN 64

4.0 CONCLUSION AND DISCUSSION 67

5.0 FUTURE PROSPECTIVE..... 70

6.0 APPENDIX & ABBRETHROUGHTIONS 71

7.0 BIBLIOGRAPHY 73

LIST OF FIGURES

Figure 1. Overview of autophagy process. 16

Figure 2. Overview of p62-involved autophagy process. 19

Figure 3. p62 domains 20

Figure 4. Autophagy-related genetics study in Parkinson's disease (PD). 25

Figure 5. Autophagy-related genetics study in Huntington's disease (HD). 27

Figure 6. Autophagy-related signaling pathway study in Alzheimer's disease (AD). 29

Figure 7. Reported crystal structures of p62 domains. 30

Figure 8. Workflow of Swiss-Model. 32

Figure 9. Parameters setting in SYBYL. 34

Figure 10. Workflow of Z-DOCK 37

Figure 11. Homology model of full-length of p62 and the binding conformation of XIE-2008 in the ZZ domain of p62. 42

Figure 12. Intermolecular view of p62 binding between its LIR domain and LC3. 44

Figure 13. Intermolecular view of p62 binding with ubiquitin through its UBA domain. 47

Figure 14. Intermolecular view of p62 binding with PKCζ through its PB1 domain 51

Figure 15. Intermolecular view of p62 binding with RIP1 through its ZZ domain 55

Figure 16. Intermolecular view of p62 self-oligomerization through its PB1 domain (Conf 1). 60

Figure 17. Intermolecular view of p62 self-oligomerization through its PB1 domain (Conf 2). 63

Figure 18. Normalized DCCs obtained by using Gaussian Network Model. 65

Figure 19. Overview of scheme of this thesis. 70

LIST OF TABLES

Table 1. Important residues in LC3-LIR binding. 45

Table 2. Important residues in Ubiquitin-UBA binding. 49

Table 3. Important residues in PKCζ-PB1 binding. 54

Table 4. Important residues in ZZ-RIP1 binding. 58

Table 5. Important residues in PB1-PB1 binding (CONF 1). 61

Table 6. Important residues in PB1-PB1 binding (CONF 2). 64

PREFACE

I sincerely appreciate my advisor, Dr.Xiang-Qun, Xie, whose instructions and support from the very beginning when I came to the University of Pittsburgh to the present time. He trained me a lot in the academic projects and communicative skills.

I am deeply grateful to my co-advisor Dr. Zhiwei Feng. He met me twice a week in the past two years and spent a lot of time discussing with me about my ongoing projects. He gave me a lot of detailed and useful suggestions, which broaden my horizons about the pharmacy research. He often assigns me projects, making me work hard and knowing how to do time management. Importantly, he trained me a lot in scientific writing and research design, which cultivate my independent thinking style and it would be important to my future research.

I would like to thank my committee members, Dr. Xiang-Qun Xie, Dr. Levent Kirisci, Dr.Jaden Jungho Jun and Dr.Zhiwei Feng. Their precious advice enlightened me and assisted me to complete my thesis.

I would like to thank Dr. Lirong Wang, Dr. Junmei Wang, who taught me a lot in practice skills and gave me a good lecture about pharmacometrics and system pharmacology.

I would like to thank all the members in Dr. Xiang-Qun Xie's lab, who kept me accompanied in the past two years and gave me a lot of help in study and life.

Last but not least, I will show my gratefulness to my parents who support me financially to complete my two-year master program. Definitely, the words "thank you" are far less enough to express my emotion in this very moment.

I offer my warmest regards and sincere blessings to all of those who helped me during the completion of this project in any respect.

1.0 INTRODUCTION

1.1 p62: AN INDUCER OF AUTOPHAGY

Autophagy is a term of the ancient process in eukaryotic cells to target the cytotoxic materials to the lysosomes and then degrade those materials though lysosome hydrolyses.(1) Cytotoxic materials could be considered as misfolded protein aggregates, pathogens, or the damaged mitochondria. Autophagy usually initiates when the cells are under metabolic emergencies and is an evolutionarily conserved lysosomal pathway related to cell survival. This 'self-digestion' behavior in cells could result in firstly, providing cells with intracellular energy when cells are lacking nutrition, for example, in the progress of cancer; Secondly, removing the waste or performing the detoxification in the prevention of endoplasmic reticulum (ER) and oxidative stress, which can occur mostly when misfolded proteins and dysfunctional organelles exist. In general, as shown in **Fig. 1**, the autophagy process involves the following steps: initiation and phagophore nucleation, phagophore expansion, cargo sequestration, membrane sealing, autophagosome maturation, fusion with lysosome, and degradation.(2) Autophagosome, a kind of cytosolic double-membrane vesicle will uniquely form in the process of the macro autophagy. Then autophagosomes would fuse with lysosomes to degrade contents and then recycled.

The discovery of the key autophagic factors like autophagy-related ('ATG') proteins, ULK1, WIPI2, beclin1, and some autophagy receptors (p62, OPTN, NBR1 and NDP52) have accelerated the research on autophagic underlying mechanism.(3) These factors play an important role regulating autophagy process through different signaling pathways, which facilitates elucidating the indispensable roles of autophagy in various biological processes. Thus, autophagy

has been shown as a potential therapeutic target in cancer, neurodegenerative diseases and balancing inflammation.(4-6) Several signaling pathways such as PI3K/Akt/mTOR and AMPK pathway have been reported to regulate autophagy.(7) PI3K/Akt/mTOR axis is the suppressor of autophagy but a promotor of tumor cell growth, proliferation and survival.(8) Many proteins such as Atg4c, LKB1, nuclear p53 and AMPK have been reported to be a promotor of autophagy but a suppressor of tumor cell growth, proliferation and survival.

Importantly, autophagy has been reported to facilitate the clearance of misfolded protein aggregation which could be the main reason for many neurodegenerative diseases. The promotion of autophagy could provide new ideas for the therapy of these diseases, which will be discussed in **Section 1.3**.

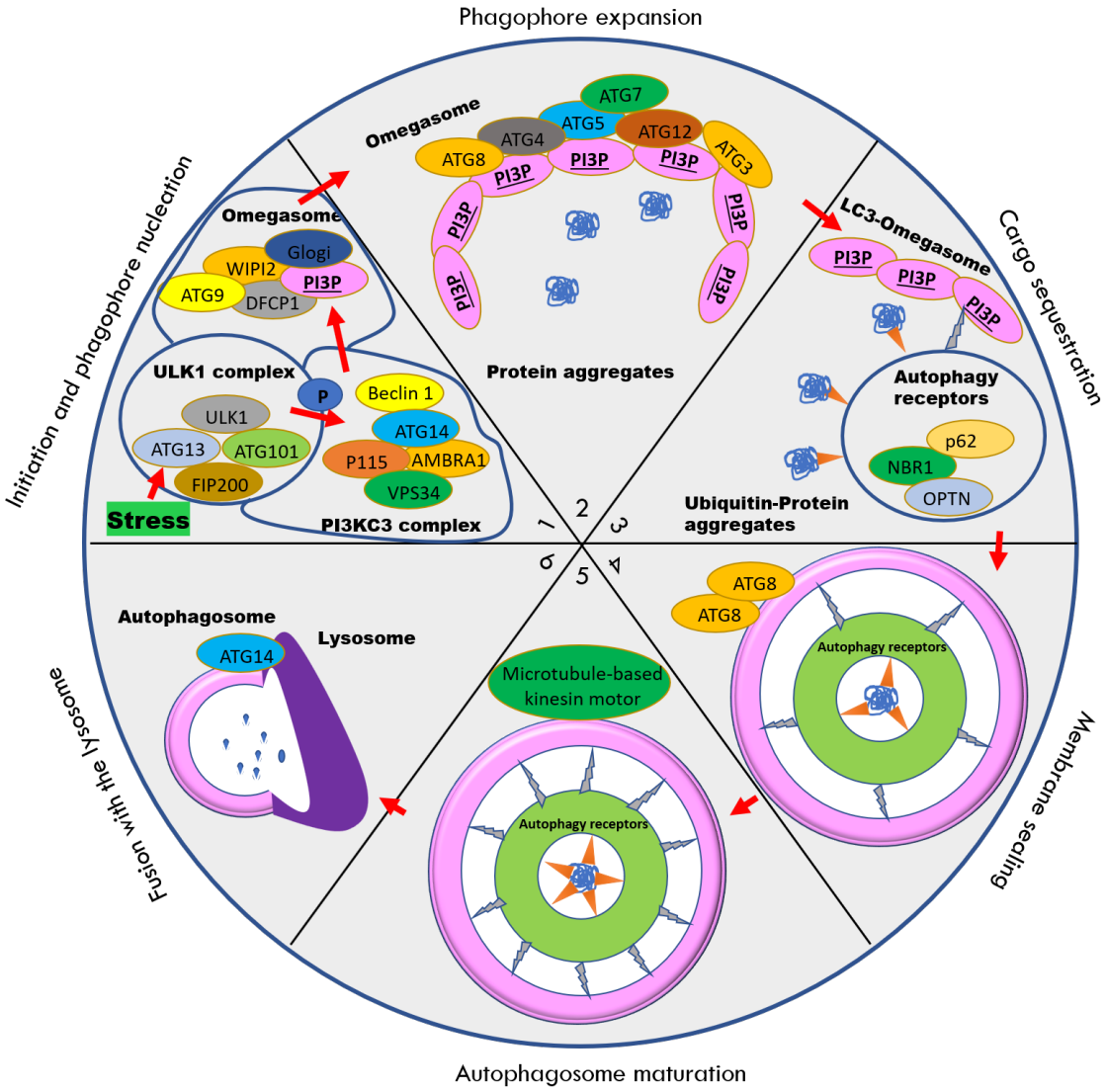

Figure 1. Overview of autophagy process.

Six steps of autophagy are: initiation and phagophore nucleation, phagophore expansion, cargo sequestration, membrane sealing, autophagosome maturation, and fusion with lysosome. 1) At first, intercellular stress leads to the formation of ULK1 complex. ULK1 complex is responsible for phosphorylating components of PI3KC3 complex, which could further facilitate the formation of omegasome by collecting other membrane sources like glogi. 2) Then with the help of ATG proteins, omegasome will expand and prepare to bind with protein aggregates. 3) Autophagy

receptors such as p62 will be involved in this step. with the help of LC3 and ubiquitin, protein aggregates will connect with the omegasome and form the cargo. 4) With all the materials prepared, cargo will gradually form the autophagosome and in particular, ATG8 participate in forming the autophagosome. 5) Autophagosome will become mature along with the ATG8 on the surface disappearing and connecting with microtubule-based kinesin motors. 6) Mature autophagosome will be transported to the targeted area. Lysosome will fuse with it and be responsible for degrading it.

p62, originally identified in 1996 by Joung et al., is the first protein identified as the autophagy adaptor between the autophagic machinery and its substrates.(9) In addition, p62 was recognized as an autophagy inducer. Importantly, the underlying mechanisms of p62-involved autophagy accompanied with cargo formation has been reported.(10-12)

As is shown in the **Fig. 2**, the first step of p62-involved autophagy process is p62 connecting or carrying with the degraded proteins. p62 combines ubiquitin-proteasome system (UPS) with autophagy process.(13-16) p62 could mediate the crosstalk between autophagy and the ubiquitin-proteasome system through N-degrons, such as Nt-Arg.(17) This is supported by the evidence that HeLa cells without p62 could not form the autophagy response even if the cell was under the proteasome inhibited condition.(18) The C-terminal ubiquitin-binding domain (UBA) of p62 is used as the adaptor to link the p62 with misfolded and ubiquitinated proteins, which forms cargos called ‘p62-bodies’.(19) Then the cargos would be delivered to the autophagosomes in the next step. P62 interacts with ubiquitin through lysine residues in position 48 and in position 63, whose binding affinity would increase due to the caseine kinase 2 (CK2)-mediated phosphorylation of serine 403.(20, 21) However, if some misfolded proteins accumulate to form

the aggregates, the ubiquitin-proteasome system will be inhibited, and this system is not able to eliminate those proteins. At this point, increased cytosolic R-BiP would be caused by reduced UPS activity and interact with ZZ domain to achieve one "open active state" of p62. This will lead the p62 accumulation and further oligomerization through PB1 domain to form aggregates. The aggregation facilitates the binding between LIR domain and LC3, which could assist cargos delivery to the autophagosomes. In one word, p62 activates the autophagy when the ubiquitin-proteasome system was retarded.(17)

In next step, p62-mediated transportation of p62-cargos targets into autophagosomes specifically. The LC3 binding with the autophagosome plays an indispensable role in elongating and closing the autophagosome. In detail, a C-terminal glycine residue of the LC3 protein should be exposed and conjugated to a phosphatidylethanolamine (PE) group to form LC3-II, called the maturation of LC3 protein. When the ubiquitin-proteasome system was inhibited as mentioned above, LC3 expression will increase. The LC3 in the autophagosome could be recognized by the LIR domain in the p62, resulting in the direct and specific connection between p62-cargos and autophagosome. However, this interaction would be dependent on the ubiquitination of soluble cytosolic proteins or organelles. Simultaneously, LC3 is also necessary for the formation of p62 cargos, which was validated by the LC3 knock down assay.(19, 22-24)

Except the pathways combining the autophagy and ubiquitin-proteasome system (UPS), some proteins could be degraded by p62 in an autophagy-independent pathway without UPS. For example, STAT5A_ΔE18 aggregates do not have the ubiquitinated residues, but p62 is responsible for the clearance of this kind of protein through its PB1 domain.(19)

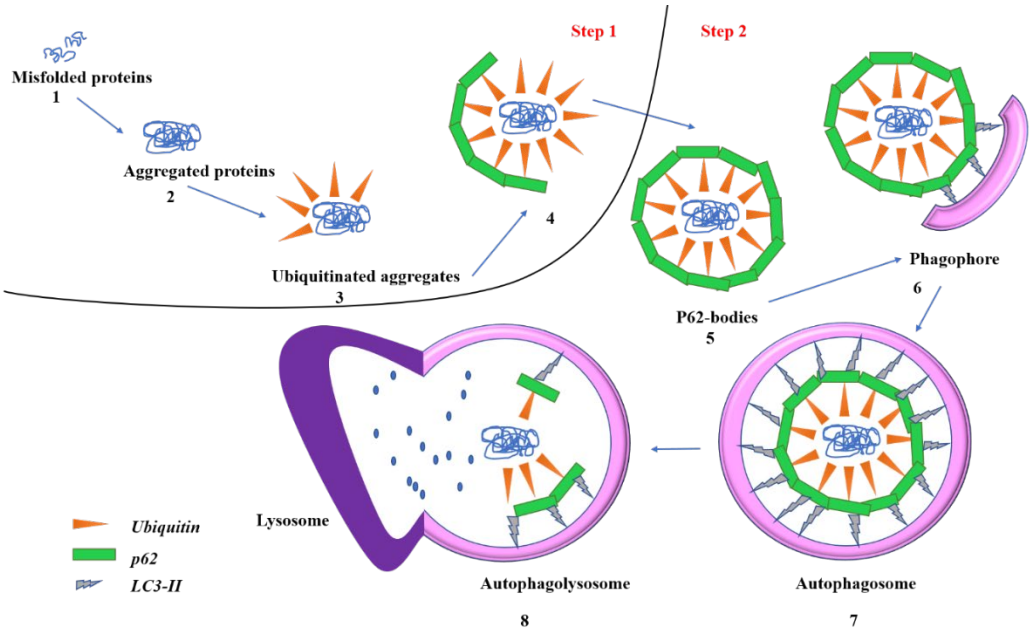

Figure 2. Overview of p62-involved autophagy process.

Misfolded protein aggregates will bind with the ubiquitin which marked as orange triangles. The UBA domain of p62 (marked as the green rectangular) would recognize the ubiquitinated aggregates to form the p62 bodies. Then phagophore will form finally with the help of LC3 (marked as gray lightning markers) on the omegasome. After the expansion of phagophore, autophagosome will mature and then transport the lysosome.

1.2 FUNCTIONAL DOMAINS OF p62

p62, which is also called sequestosome 1 or ZIP3, is a multi-domain scaffold protein participating in several signaling pathways of the antioxidant response, inflammation, etc. Six major domains of p62 have been reported, including an N-terminal Phox1 and Bem1p (PB1) domain (aa. 1-102), a zinc finger (ZZ) domain (aa. 121-167), TRAF6-binding (TB) domain (aa. 228-256), an LC3-interacting region (LIR) domain (aa. 332-344), a Keap1-interacting region (KIR) domain (aa. 347-357) and a ubiquitin-associated (UBA) domain (aa. 391-433). (**Fig. 3**)(25, 26)

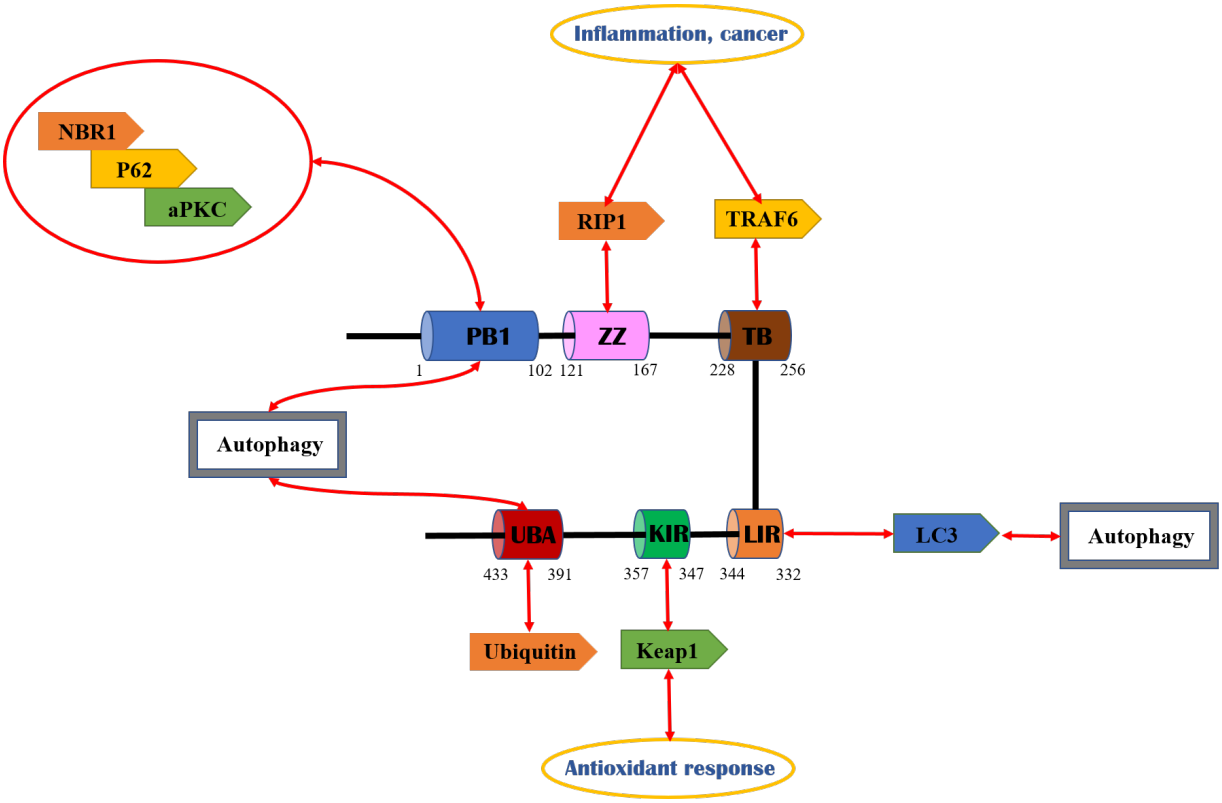

Figure 3. p62 domains.

p62 has six known domains which are PB1, ZZ, TB, LIR, KIR and UBA. The number of amino residues of each domain has been shown in the **Fig. 3**. Six domains are represented by six cylinders

in different colors. The known partners of each domain have shown as rectangles of different colors. The interactions between these partners and domains of p62 (marked as red bidirectional arrow) play an indispensable role in different physiological symptoms (marked in the yellow circles). PB1 (blue), UBA (red) and LIR (orange) domain of p62 are related to the regulation of autophagy. ZZ (pink) and TB (brown) domain of p62 are related to the inflammation and cancer. KIR (green) domain is considered as the regulator of antioxidant response in cells.

Importantly, PB1 is capable of homodimerization and heterodimerization. p62 PB1 domain has both a basic front end and acidic rear end (A-B type PB1 domains). “A-type” PB1 domains have conserved acidic residues, and “B-type” PB1 domains have a conserved lysine or arginine in the basic region. PB1 domains have α-β grasp topology in the front end which could bind with the back end of the other PB1 domain. Among p62 domains, Phox1 and Bem1p (PB1) domain interacts with PB1 domains of the other proteins such as atypical protein kinases C, MEK5, NBR1 protein and ERK, which are called the partners.(27) The binding with these partners is dependent on the front end of the p62, but not the rear end acidic cluster region. The partners such as the MAPK kinase, and MEKK3 bind with the rear end acidic cluster region. The p62-MEKK3 complex is related to TRAF6-regulated NF-κB signaling and the assembly of polyubiquinated proteins sorting to sequestosomes and proteasomes. NF-κB signaling is a response to neurotrophic factors and inflammatory cytokines, including IL-1 and tumor necrosis factor, which indicate the p62 could be related to these factors mediated important physiological processes. MEKK3 could also phosphorylates and activates the MAPK, ERK5, and MEK5 through PB1 domain. In addition, the binding between atypical PKCs and PB1 of p62 activates the transcription factor NF-κB downstream of cell stimulation by interleukin 1 (IL-1), RANK ligand (RANKL), or nerve growth

factor (NGF). On the other hand, the binding between ERK1 and PB1 could inhibit the ERK activity and then modulate adipogenesis. This was supported by the evidence that p62 knock-out mice are insulin-resistant and obese as a result of a loss of ERK1/2 regulation in adipogenesis. P62 interaction with MEK5 through PB1 domain promotes not only the ERK5 binding with p62, but also the recruitment of TRAF6 to the mammalian target of rapamycin complex 1 (MTORC) complex. This influence on the mTOR pathway could result in the elevated level of c-Myc and the inhibition of autophagy-related functions. (28, 29)

ZZ zinc finger domain of p62 is also very important for self-oligomerization and degradation of p62. Experiments have shown that p62 aggregation could be induced by the binding of p62 ZZ to Nt-R substrates. p62 could also activate mTORC1 pathway activation through ZZ domain in response to arginine. In addition, zinc finger (ZZ) domain interacts with the serine/threonine kinase 1 (RIP1).(30, 31) RIP1 is involved in PI3K/Akt (phosphoinositide 3-kinase/ protein kinase B)-forkhead pathway, death receptor-mediated mitogen-activated protein kinases (MAPK) pathway, Toll-like receptor (TLR) 3 and TLR 4-mediated cell survival signaling, and genotoxic stress-induced activation of NF-κB, apoptosis.(32, 33) Interruption of RIP1 connection with the ZZ domain of p62 could inhibit both the activation of cell proliferation, NF-κB signaling pathway and autophagy.(30, 34-36) Our lab reported that p62 ZZ ligands (XIE62-1004 and XIE2008) can accelerate autophagic degradation of mutant huntingtin (mHTT) proteins to treat the Huntington's disease, a neurodegenerative disorder.(17) Moreover, we also reported another p62-ZZ inhibitor, XRK3F2, can inhibit multiple myeloma (MM) cell growth.(37)

TNF receptor-associated factor 6 (TRAF6) is an important partner of the TB domain. This interaction could facilitate the p62 oligomerization and result in K63 polyubiquitination of TRAF6

leading to the activation of NF-κB. The p62-TRAF6 complex appears to regulate both phosphorylation and ubiquitination of the IKK complex.(25)

A new region between the ZZ and TBD domains which is responsible for p62 binding with the mTOR regulator Raptor has been reported.(38) mTOR consists of two distinct complexes in mammalian cells. One is mTORC1 which is formed by the mTOR, Raptor and GβL proteins. Another one is mTORC2 which is formed by mTOR, Rictor, mSin1, GβL and Protor. mTORC1 could respond to amino acids, stress, oxygen, energy, and growth factors and is acutely sensitive to rapamycin. mTORC1 is highly sensitive to the nutriment deprivation that leads to the inactivation of the serine/threonine kinase mTOR. It promotes cell growth by inducing and inhibiting anabolic and catabolic processes, respectively, and also drives cell-cycle progression. mTORC2 responds to growth factors and regulates cell survival and metabolism, as well as the cytoskeleton. mTORC2 is insensitive to acute rapamycin treatment but chronic exposure to the drug can disrupt its structure. The middle panel describes the known functions of the protein components that make up the mTOR complexes and the bottom panel schematically depicts their interaction sites. mTORC1 is dependent on the uptake of amino acids that participate in the lysosomal membrane localization of mTORC1 to promote Rag GTPase-mediated mTOR activation.(39, 40)

The p62 is degraded by selective autophagy through LIR, a region connecting p62 with the autophagy regulator LC3, which aims to keep the cytosol away from the mutated and misfolded proteins. LC3-I would convert to the LC3-II on the autophagosomes' membranes and LC3-II could be degraded by the lysosome. p62 forms the protein bodies containing the LC3 and then is degraded.(41)

Another key domain related to the aggregate formation and autophagic clearance is UBA. UBA domain is a C-terminal region of p62 composed of a three-helix bundle of 50 amino acids. It has been reported to target at the polyubiquitinated proteins and then transport them for proteasomal degradation.(42)

p62 interacts and inhibits the Keap1 through its KIR domain inducing the activation of erythroid 2–related factor 2 (NRF2)-dependent oxidative and electrophilic stresses response. Keap1 is a component of Cullin-3-type ubiquitin ligase for Nrf2. NRF2-Keap1 system is formed by two Keap1 molecules and one Nrf2 molecule. The animal experiments show that elevated Nrf2 level could lead to the toxicity in autophagy-impaired livers.(43)

1.3 p62 IN NEUROGENERATIVE DISEASES

1.3.1 REGULATION OF p62 IN PARKINSON'S DISEASE (PD)

Parkinson's disease (PD) is the second most common neurodegenerative disorder that leads to shaking, stiffness, and difficulty with walking, balance, and coordination. As the disease progresses, they may also have mental and behavioral changes, sleep problems, depression, memory difficulties, and fatigue. Parkinson's disease occurs when nerve cells, or neurons, in an area of the brain that controls movement become impaired and/or die and produce less dopamine than normal state.

Parkinson's disease genetic studies have identified that mutations in genes are associated with increased risk for developing PD.

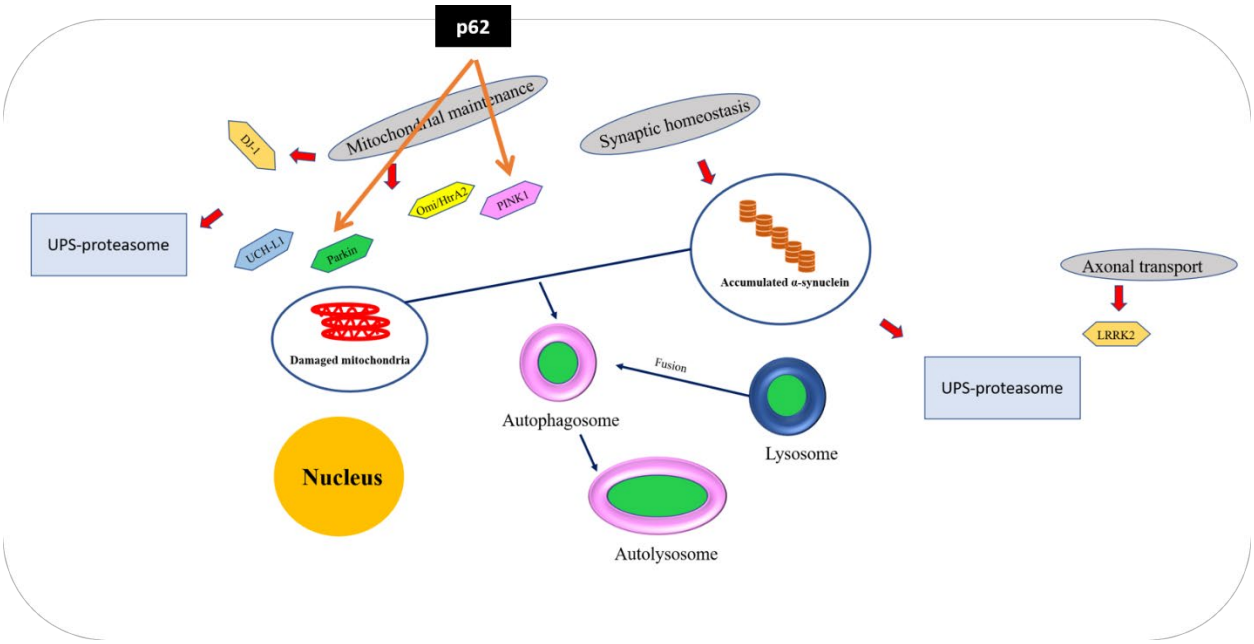

Figure 4. Autophagy-related genetics study in Parkinson's disease (PD).

PD is usually caused by the accumulation of α-synuclein (α-syn).(44) There are some reported genes which plays an important role in pathogenesis of PD. Autophagy contributes to transporting and degrading damaged mitochondria and accumulated α-syn.

ATG genes like PARK2/Parkin and PARK6/PINK1 PARK7/ DJ-1 have been reported to be associated with the defective autophagy (autosomal recessive or sporadic early-onset Parkinson's disease) through mitophagy induction, which has been proved by the gene mutation experiments.(45, 46) Mitophagy is the selective degradation of mitochondria by autophagy. There are three potential ways PINK1/Parkin effecting autophagy: 1) PINK1 and Parkin may regulate mitochondrial size by affecting fusion and fission, allowing fragmented mitochondria to be taken up in autophagic vesicles. 2) PINK1 and Parkin may skew the movement of mitochondria towards the autophagosome- and lysosome-rich perinuclear area. 3) PINK1 and Parkin may directly recruit

the autophagic machinery to damaged mitochondria for degradation. Scientists reported that p62/SQSTM1 is indispensable for Parkin-induced mitochondrial clustering (47) and plays a role in PINK1/Parkin-mediated mitophagy. (48)

In addition, observations in PD brain tissue suggest an aberrant regulation of autophagy associated with the aggregation of α-synuclein (α-syn) and autophagy is one of the main systems involved in the proteolytic degradation of α-syn. p62 has been reported to regulate α-syn aggregation in PD.(49)

1.3.2 REGULATION OF p62 IN HUNTINGTON'S DISEASE (HD)

Huntington's disease (HD) is an autosomal dominant neurodegenerative disorder characterized clinically by chorea, cognitive decline and psychiatric symptoms.(50) The main cause of this disease is a dominantly inherited expansion of a CAG repeat (more than 37 repeats) within the coding region of the huntingtin (HTT) gene that generates an aberrant and misfolded protein. This protein aggregates and forms inclusion bodies, which is the neuropathological feature of HD.(51, 52) Autophagy can assist the degradation of mHTT. This is suggested by the fact that ATG7 is necessary for lipidation of LC3, and lacking ATG7 could be related to neurodegeneration. A polymorphism in ATG7 happens on the early stage of HD.(53)

p62 is reported to be associated with HD through mediating autophagy and clearance of aggregated mutant huntington under stress and it can be the potential treatment of HD. From the observation of the caudate nucleus from HD patients, mRNA expression of LC3A, ULK2, and LAMP2 is significantly increased, but PTEN-induced kinase 1 (PINK1), WDFY3 or ALFY, and

FK506-binding protein 1A (FKBP1A) are significantly decreased.(54, 55) Upregulation of the IKK (inhibitor of κB kinase) complex mediating S13/S16 phosphorylation increases the expression several genes in the ubiquitination pathway and leads to increased autophagic and proteasomal HTT degradation. mHTT fragments could bind with K63 preferably, and p62 was suggested to bind with the K63-ubiquitinated mHTT fragments to be targets for autophagy.(54)

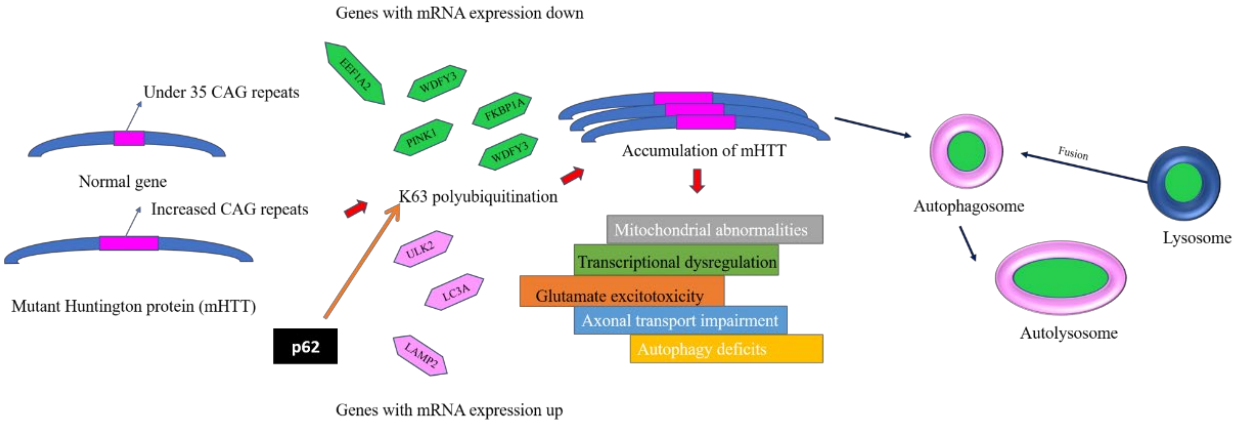

Figure 5. Autophagy-related genetics study in Huntington's disease (HD).

HD is usually caused by the accumulation of mutant Huntington protein (mHTT). There are some reported genes which plays an important role in pathogenesis of HD. Autophagy contributes to transporting and degrading mHTT.

1.3.3 REGULATION OF p62 IN ALZHEIMER'S DISEASE (AD)

AD is the most common neurodegenerative disease and most common cause of dementia. It is a progressive disorder that slowly destroys memory and cognitive functions. The pathological

mechanism of AD is still unclear. There is growing evidence to indicate that mitochondrial dysfunction plays a crucial role in the pathogenesis of AD.(56) The function of p62 in mitophagy suggest that the p62 is involved in Alzheimer's disease (AD) pathology. Tau is a major microtubule-associated protein found in brain, located mainly in the axons of neurons. Tau protein is subject to multiple phosphorylations and subsequently it aggregates into neurofibrillary tangles.(57) There are three facts showing that p62 is associated with AD. Firstly, p62-deficient mice possess AD tau brain pathology associated with learning and memory deficits and neurodegeneration. In addition, p62-deficient brain has less Nrf2 nuclear localization, which is like AD brain. Interestingly, AD brain exhibits reduced levels of p62.(58)

Nrf2 level in the nucleus was shown to be decreased in the brain from AD individuals. (59) Nrf2 plays a central role in the gene expression of phase II detoxification enzymes and some antioxidant genes. The transcription factor Nrf2 (NF–E2-related factor 2)-ARE pathway can be activated and be responsible for the protection cells from oxidative stress-induced cell death. Increased oxidative stress could contribute to the pathogenesis of in Alzheimer's disease. P62 was suggested to regulate Nrf2 activity but the underlying mechanism is still not clear.(59)

p62 knockout mice has shown some neuropathological lesions including the accumulation of hyperphosphorylated tau and neurofibrillary tangles, synaptic deficiencies with loss of working memory and neuronal apoptosis. In addition, the decrease in the cytoplasmic p62 would cause a major accumulation of autophagic vacuoles containing APP and β-secretase-cleaved APP in dystrophic axons and dendrites.(60, 61)

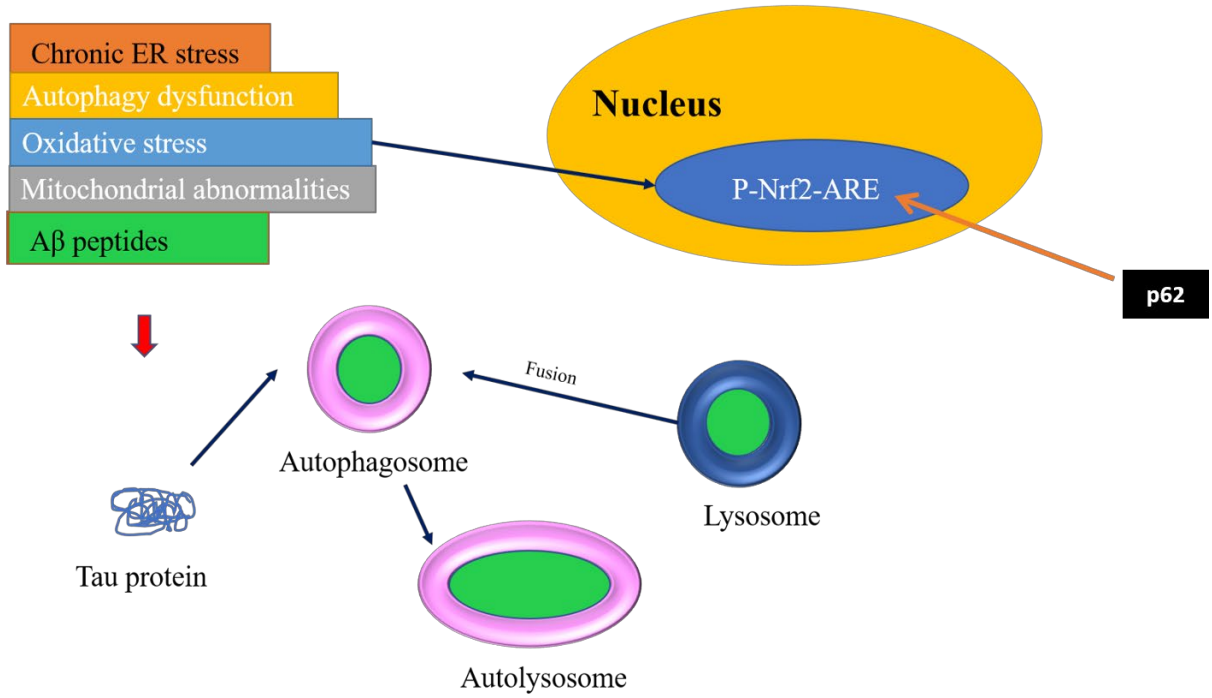

Figure 6. Autophagy-related signaling pathway study in Alzheimer's disease (AD).

AD is usually caused by the accumulation of Tau protein. There are some reported signaling pathways which play an important role in pathogenesis of AD. Autophagy contributes to transporting and degrading Tau protein.

2.0 MATERIALS AND METHODS

2.1 PREPARED DOMAINS

As is shown in the **Fig. 7**, some structures of p62 domains have been reported. They are the NMR structure (Rattus norvegicus) of PB1(62) (PDB entry: 2KKC) and the crystal structures of LIR (63) (PDB entry: 2ZJD, resolution 1.56 Å), KIR (64) (PDB entry: 3ADE, resolution 2.80

Å), and UBA (65) (PDB entry: 3B0F, resolution 1.40 Å). These structures were retrieved from the Protein Data Bank (http://www.pdb.org/pdb/), and then were prepared by SYBYL-X 1.3 (66) software for residues repair and energy minimization.

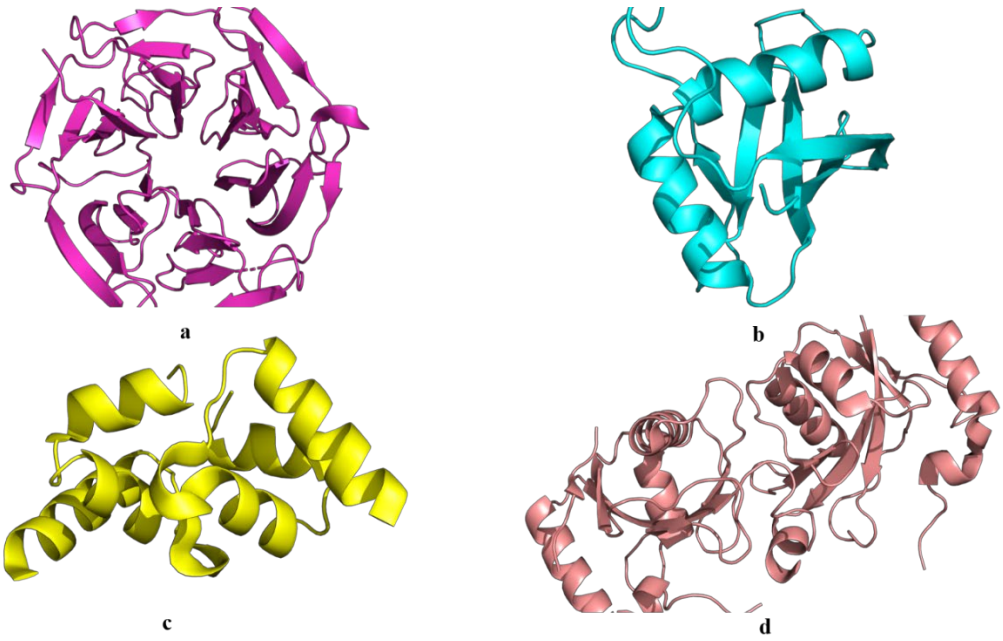

Figure 7. Reported crystal structures of p62 domains.

a. KIR (PDB ID: 3ADE) **b.** PB1 (PDB ID: 2KKC) **c.** UBA (PDB ID: 3B0F) **d.** LIR (PDB ID: 2ZJD)

2.2 HOMOLOGY MODEL

The whole sequence of p62 (Q13501 or SQSTM_HUMAN, 440 aa) was retrieved from the UniProtKB / Swiss-Prot (http://www.uniprot.org/uniprot/).

The detailed protocol for p62 3D homology modeling can be found in our recent publication.(67) Briefly, we divided the whole sequence of p62 into nine domains (and three loops) according to their functions. Then modeler was used to construct its 3D model using reported domains (mentioned in **Section 2.1**).

In order to further validate the 3D model of p62, we docked domains of p62 with their partners. PKCζ is the partner of PB1 domain of p62. Since no reported crystal structure of homo PKCζ exists, we used the SWISS-MODEL, an automated online server used for homology modeling, to build homology modeling of PKCζ. The sequence of PKCζ was retrieved from the UniProtKB / Swiss-Prot (http://www.uniprot.org/uniprot/). SWISS-MODEL used 5LI1 as template and build the homology model of PKCζ with the 84.73% identity. SYBYL-X 1.3 (66) software was used for residues repair and energy minimization.

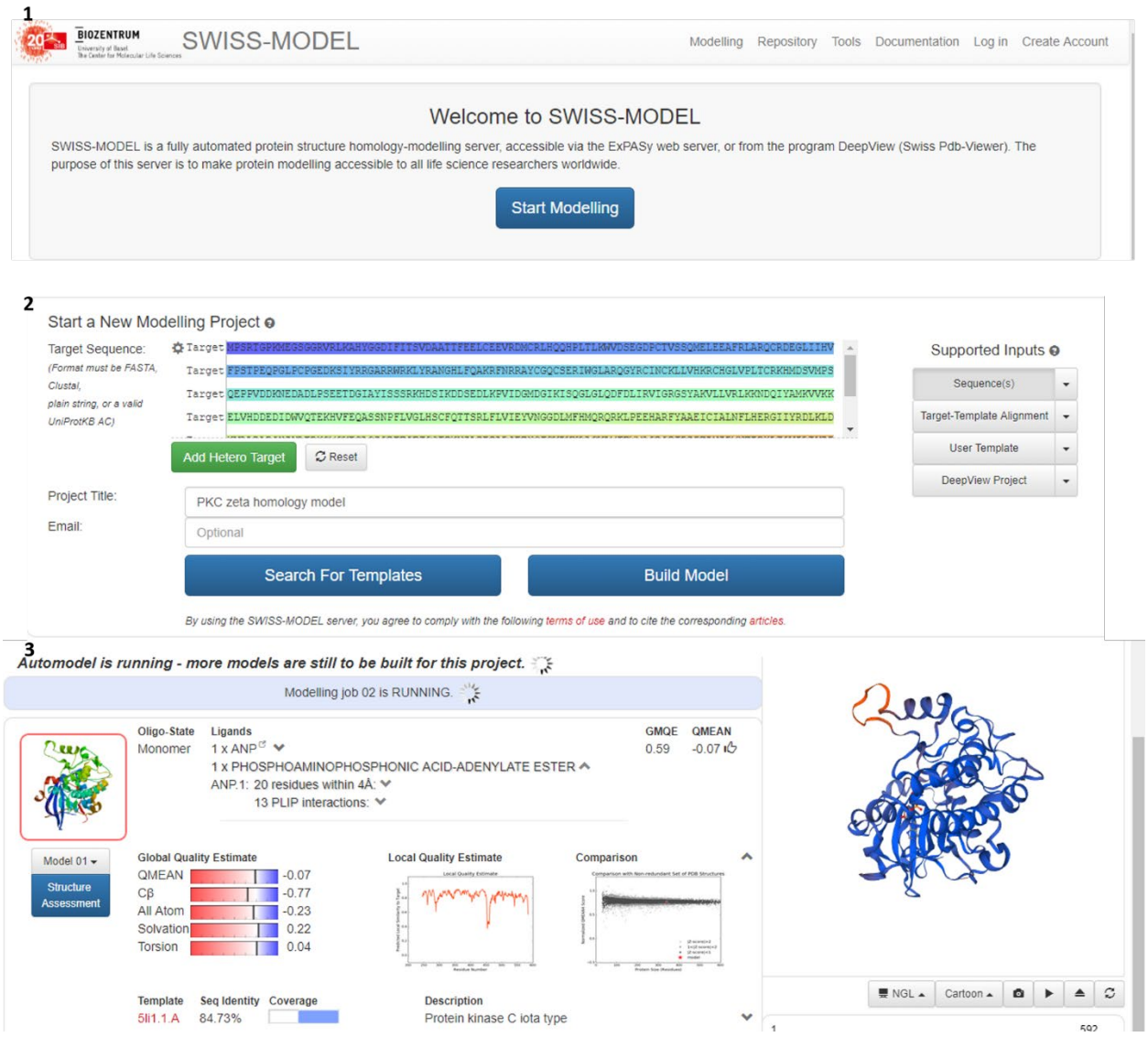

Figure 8. Workflow of Swiss-Model.

The sequence of PKCζ was retrieved from the UniProtKB / Swiss-Prot (http://www.uniprot.org/uniprot/). From this procedure, we obtained the final model and its template with highest identity.(68)

2.3 DOCKING

2.3.1 SYBYL DOCKING

The first one was about the docking study with XIE-2008,(67) our synthesized small molecule to the p62 ZZ domain. We used Surflex-Dock GeomX (SFXC) in SYBYL-X 1.3(66) to perform the docking, in which the total Score was expressed in -log10(Kd).(69)

As is shown in the **Fig. 9**, the main protocols or parameters(70) of this docking were as the following.

(1) The entire surface of ZZ domain (including the cavity) was regarded as the binding pocket.

(2) The Threshold was set to 0.50, while the Bloat was set to 4.

(3) Additional starting conformations per molecule was set to 10.

(4) Max number of rotatable bonds per molecule was set to 150.

(5) Maximal number poses per molecule was set to 200.

(6) Density of search was set to 9.0 and number of spins per alignment was set to 20.

(7) Pre-dock minimization, post-dock minimization, molecule fragmentation, ring flexibility and soft grid treatment were turned on.

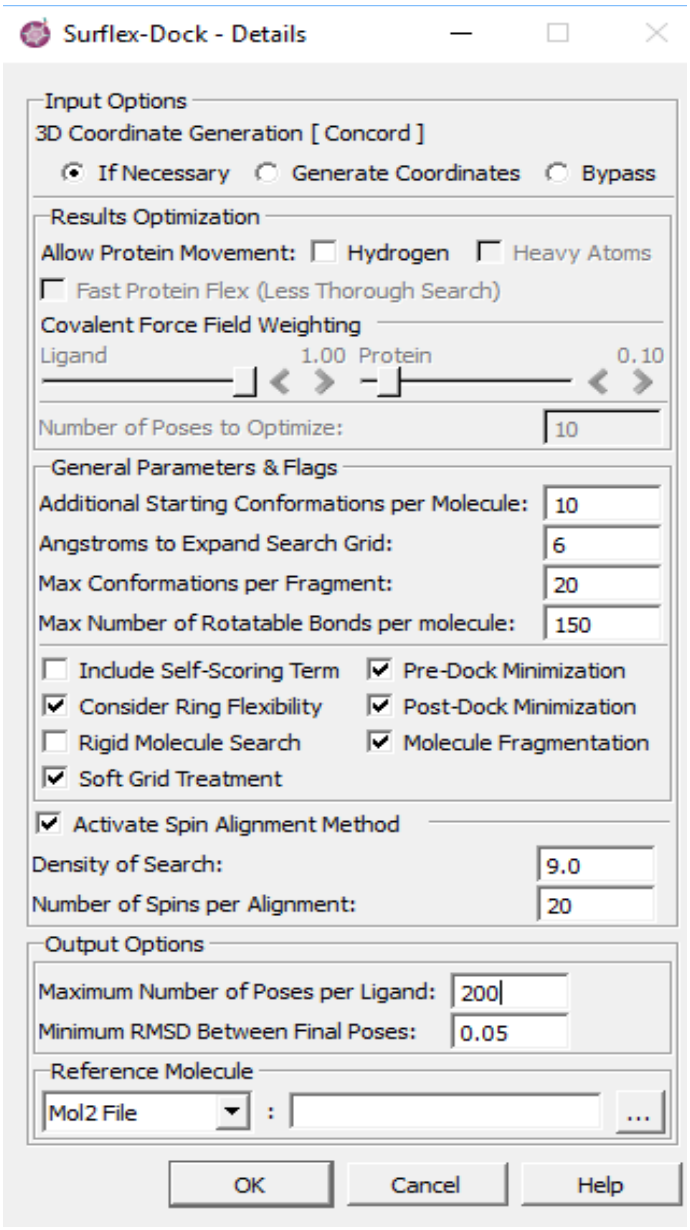

Figure 9. Parameters setting in SYBYL.

We changed the default parameters. Additional starting conformations per molecule was changed to 10 and maximum number of poses per ligand was changed to 200.

2.3.2 Z-DOCK

We first attempted to submit the whole structure of p62 and LC3 / Keap1/ λPKC / ubiquitin to Cluspro-2.0 (71) sever, GRAMM-X (72) web server and ZDOCK (73) server for predicting the interactions. However, these servers failed to predict any reasonable the interactions, even when we defined the contacting and blocking residues.

We then used another protocol. Instead of submitting the whole protein of p62, we selected the reported domains (LIR for LC3, KIR for Keap1, PB1 for λPKC, and UBA for ubiquitin), and also submitted some domains surrounding LIR / KIR / PB1 / UBA for docking. Details can be found in the following paragraph.

We used ZDOCK (73) to perform this type of docking study. ZDOCK was a rigid-body docking program, which used a fast Fourier transform to search all possible binding modes for the protein through evaluating shape complementary, desolvation energy, and electrostatic. We superposed the domains from docking results with our original structure of p62 and confirmed no conformational changes (rigid) for the docking domains.

As is shown in the **Fig. 10**, the main protocols used for docking and used to construct the complexes of LC3 / Keap1 / PKCζ / ubiquitin and our four proteins described as the following.

(1) Uploaded LC3 / Keap1 / PKCζ / ubiquitin.

(2) Uploaded the domains that interact with LC3 / Keap1 / PKCζ / ubiquitin.

(3) ZDOCK version was setting to "ZDOCK 3.0.2".

(4) Picked contact and blocking residues both in LC3 / Keap1 / PKCζ / ubiquitin and the corresponding domains of p62, and then submitted the job.

(5) When finished, we obtained the TOP5 models. An alternative is to download two PDB files, log file and a script for generating the complexes, which generate up to 2000 models.

(6) Superposed the docking results with our whole structure of p62.

(7) Selected the best candidate by superposition with the crystal structure in each cluster. The uploaded docking domains from the docking results were constructed the complexes of LC3 / Keap1 / PKCζ / ubiquitin and our four clusters.

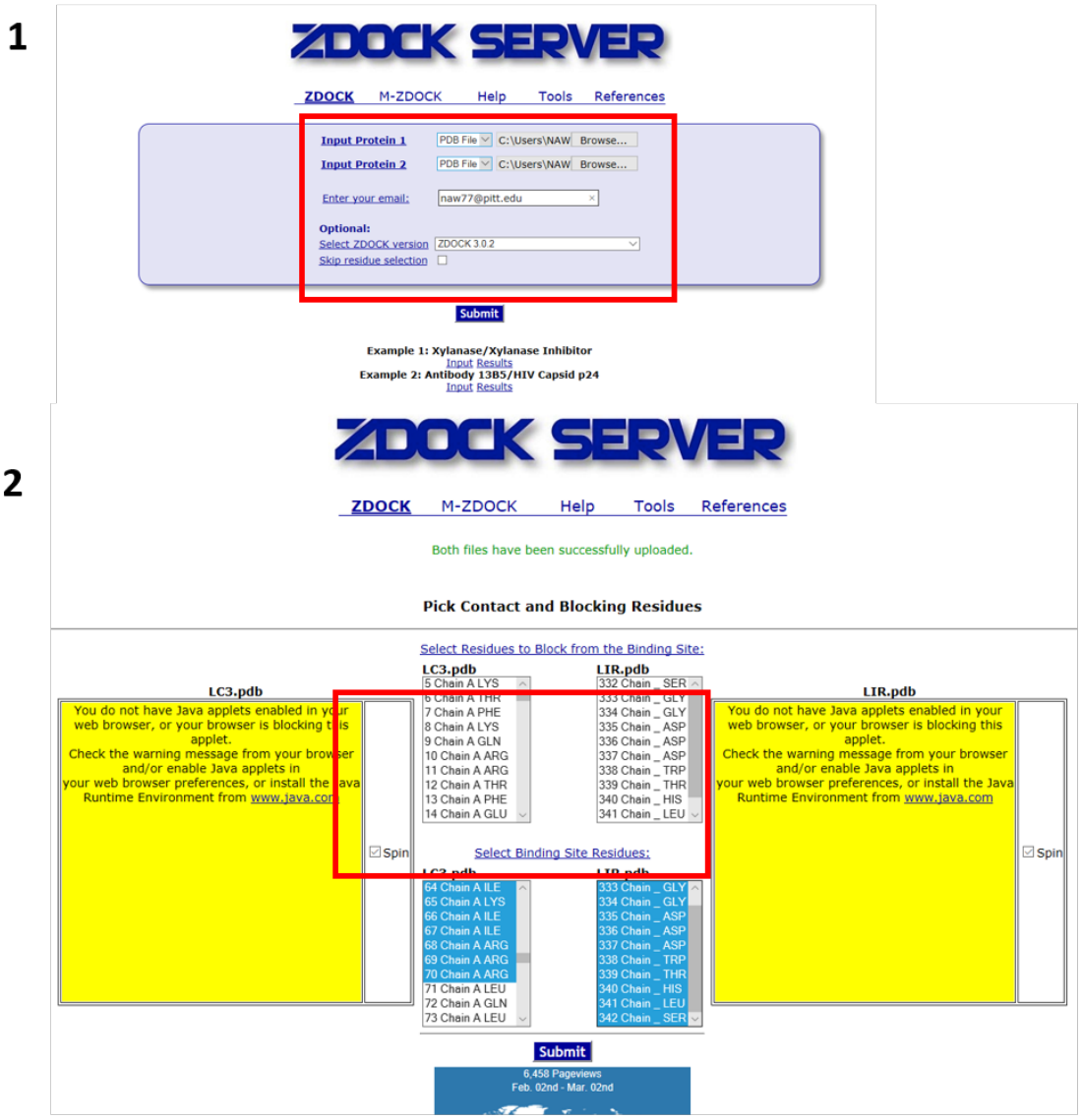

Figure 10. Workflow of Z-DOCK

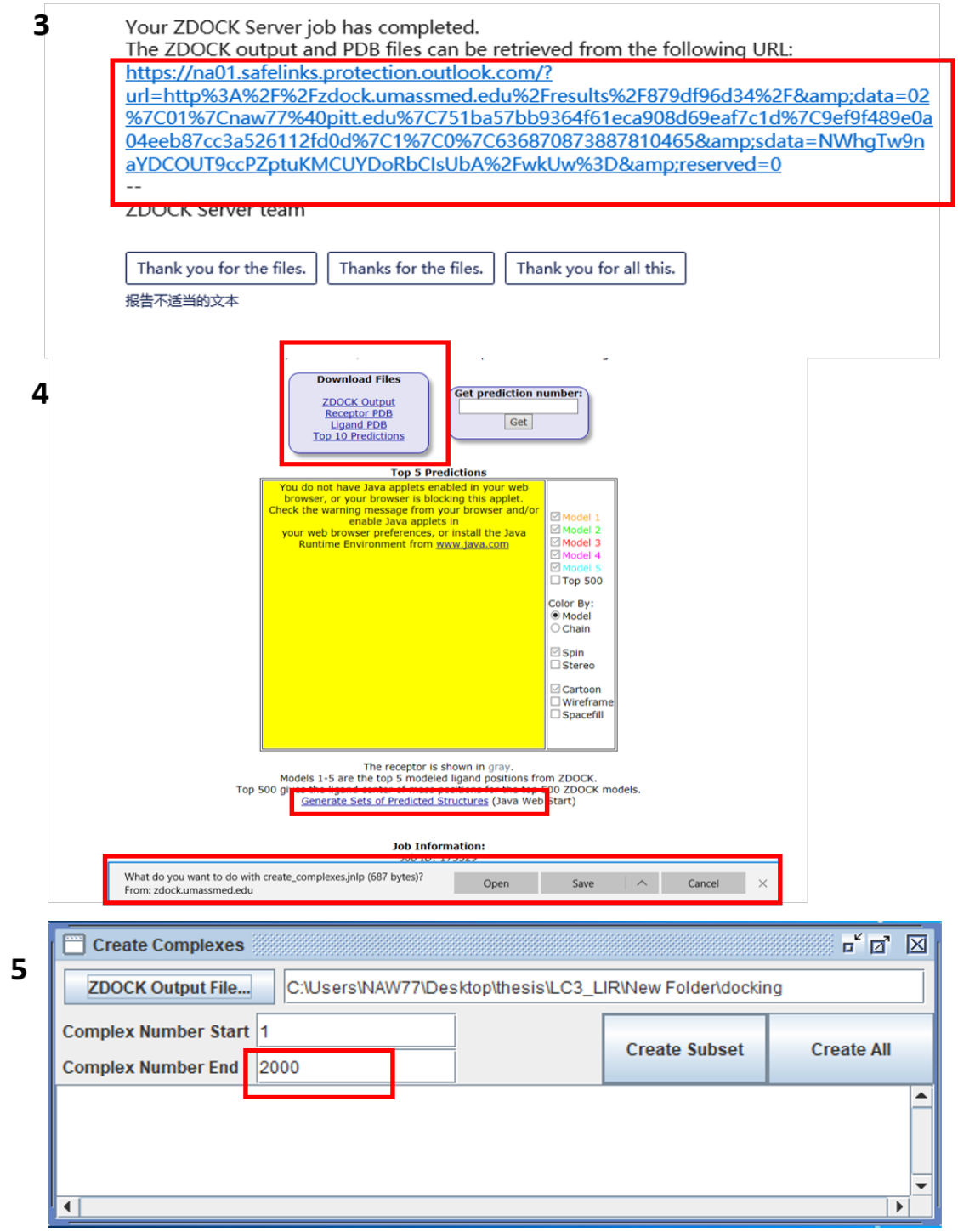

Figure 10. Workflow of Z-DOCK (Continued).

The first step is to upload the PDB files of proteins and then select the contact or blocking residues. Z-DOCK will be responsible for searching all possible modes in the translational and rotational

space between two proteins within 6 Å. Results will be sent to the e-mail address and JAVA program would be applied if users would like to see larger sets rather than top 10 results given by Z-DOCK. I chose to generate 2000 sets of results. ZDOCK is a rigid body protein–protein-docking algorithm. It fully explores three translational and three rotational degrees of freedom. The rotational space is searched explicitly, and the translational space is searched by using Fast Fourier Transform (FFT) algorithm. We used ZDOCK3.0.2, which had the most powerful scoring function compared to earlier versions of the program, by combining pairwise shape complementarity with desolvation and electrostatics. All default parameters and a 15° rotational sampling interval were used.

2.4 MOLECULAR DYNAMICS SIMULATION

Systems of full length of p62 were set up for molecular dynamics simulations using program tleap, the system was solvated into 0.15 mol/L NaCl solution, included protein 49143 water molecules, 132 Na+ ions and 132 Cl- ions. The initial configurations of protein receptors and ligands were taken from docking studies. The sizes of initial simulation boxes were ~ 124 Å * 120 Å * 125 Å.

The AMBER ff14SB force field(74) was applied to proteins and the AMBER Lipid14 force field(75) was applied to lipids. Water molecules were treated with TIP3P water model.(76) The partial atomic charges of ligands were derived by semi-empirical with bond charge correction (AM1-BCC) method.(77) The other force field parameters came from GAFF in AMBER16.(78) The residue topologies for ligands were prepared using the ANTECHAMBER module.(79)

The MD simulations were carried out using the PMEMD.mpi and PMEMD.cuda modules in the AMBER16(80-82) package. First, several minimization steps were carried out for the systems to avoid the possible steric crashes. Then, each system was gradually heated from 0K to 300K at the heating stages and then the temperature was kept at 300K at the following equilibrium and production stages. The time step of 2 fs was used for the heating, density, equilibrium and following production stages. The periodic boundary condition was employed to produce constant temperature and pressure (NPT) ensembles. Pressure was set at 1 atm and was controlled by the anisotropic (x-, y-, z-) pressure scaling protocol applied in AMBER with a pressure relaxation time of 1 ps. Temperature was regulated using Langevin dynamics with collision frequency of 2 ps-1.(83),(84) The Particle Mesh Ewald (PME) method(85),(86) was adopted to handle the long-range electrostatics and an 10 Å cutoff was set to treat real-space interactions. All the covalent bonds involving hydrogen atoms were constrained with the SHAKE algorithm.(87) The simulation time for the production stage for each system was 300 ns and the coordination of simulated systems were saved every 10 ps.

For the saved trajectories of MD simulations, Molecular Mechanics/ Poisson–Boltzmann Surface Area (MM/PBSA) binding free energies were calculated(88, 89) and free energy decompositions were performed. The interaction energies between each residue and the ligands were extracted.

3.0 RESULTS

3.1 FULL-LENGTH p62 3D STRUCTURE

The 3D structure of p62 bound with our reported compound XIE2008 was shown in **Fig. 11a**, in which we highlighted several important domains with different colors.(17) XIE2008 was reported to bind to p62 ZZ domain, in which the binding pocket composed of two distinct compartments. Asp129 and Asp149 formed the hydrophilic compartment, while Val135, Cys142, Cys145, Tyr148, Leu150, Cys151, Cys154, Leu159 formed the hydrophobic one. Asp129 (3.9 Å) and Asp149 (3.5 Å) formed strong hydrogen bond with XIE2008. Moreover, Tyr148 formed strong π-π interaction with XIE2008 (3.5 Å), while His160 interacted with XIE2008 through a strong hydrophobic interaction. In order to confirm the direct binding of XIE2008 to p62 ZZ domain, our previous work carried out pulldown assays using biotinylated-XIE2008 and full-length p62.(17) The result showed that biotinylated-XIE2008 bound to wild-type p62 but not mutants carrying point mutations within p62 ZZ domain, either D129 or C151/C154. All these details can be found in our previous work.

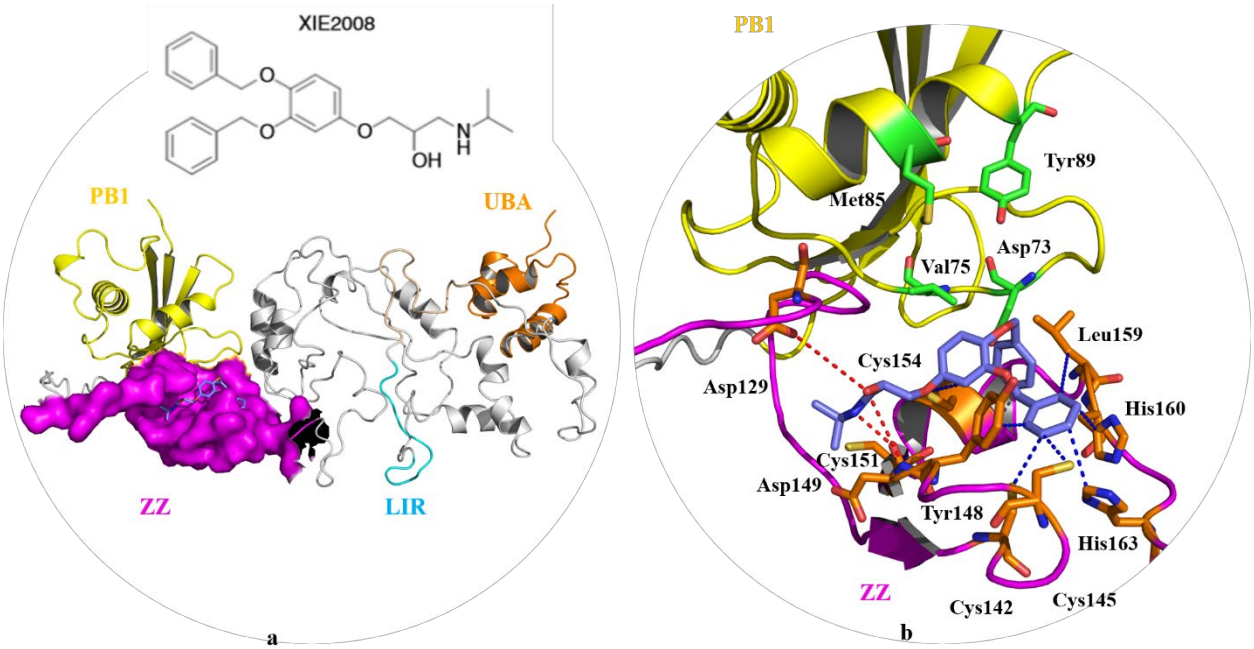

Figure 11. Homology model of full-length of p62 and the binding conformation of XIE-2008 in the ZZ domain of p62.

a. Full-length structure of p62. Each domain is shown in different colors. XIE2008 (blue) is shown to bind with the ZZ domain (magentas). PB1 domain is highlighted in yellow. UBA domain is highlighted in orange. LIR domain is highlighted in cyan. b. Zoom-in view of Xie2008 binding in the ZZ domain. XIE2008 is shown as blue sticks by elements. Important residues in the PB1 domain are shown in green, while the important residues in the ZZ domain are shown in orange. Blue dotted lines represent hydrophobic interactions while the red dotted lines represent the hydrophilic bonds.

3.2 BINDING OF p62 WITH LC3

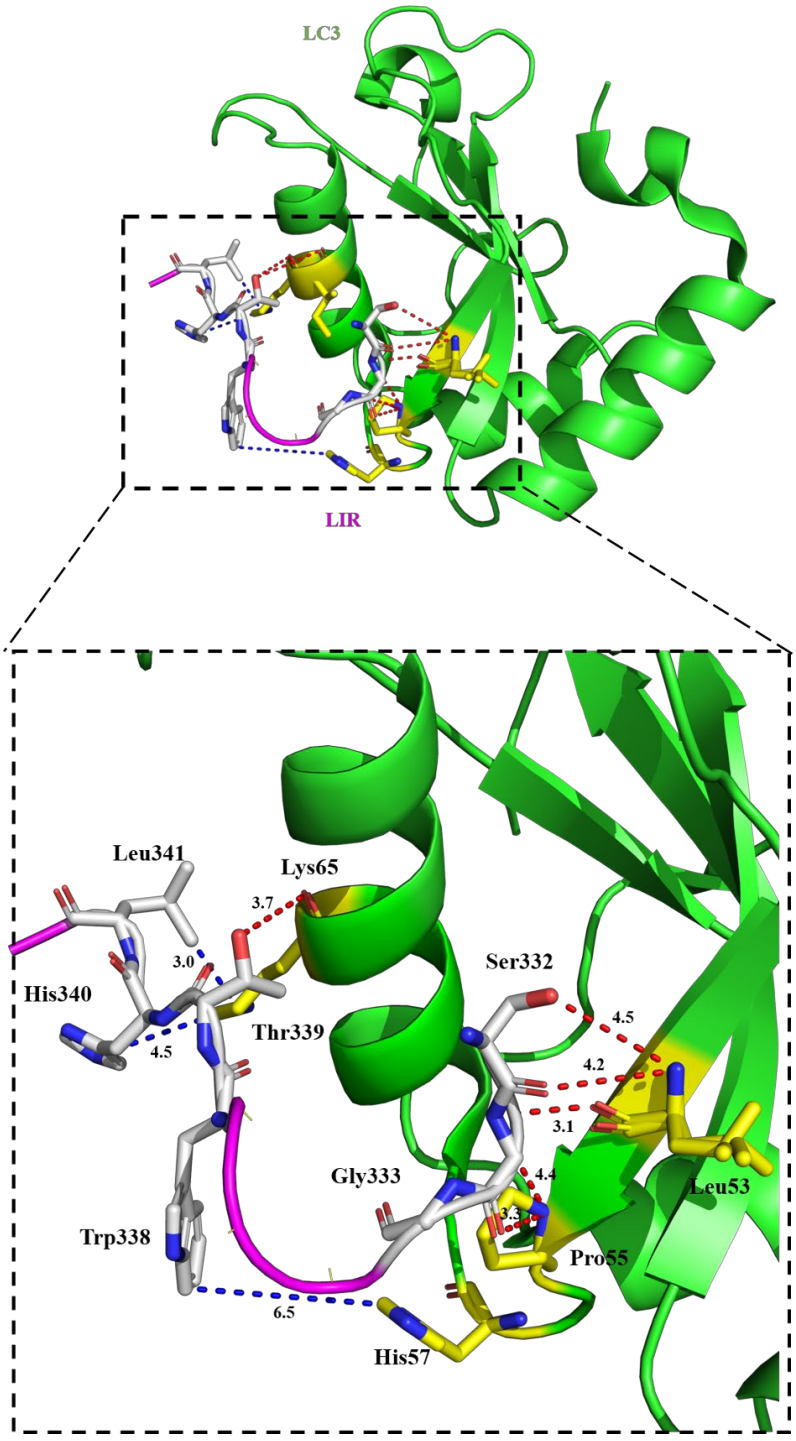

Figure 12. Intermolecular view of p62 binding between its LIR domain and LC3.

The left one shows the interactions between LIR domain (magentas) of p62 and LC3 (green). Red dotted lines represent hydrophilic bonds while the blue one means the hydrophobic interactions. Important residues from the LIR domain was marked as white sticks by elements. Important residues form the LC3 protein are shown as yellow sticks by elements. The length of predicted interaction has been marked. The right one is the zoom-in view showing the interactions clearer.

The relative orientations of our p62 LIR domain and LC3 were based on the reported crystal structure of FYCO1 (FYVE and coiled-coil protein 1) LIR domain bound with LC3. Homo crystal structure of LC3-LIR peptide complex (PDB ID: 5D94) has been reported.(90) Superimposition and adjustment were applied to obtain an accurate complex. Briefly, our LIR domain of p62 was superimposed onto the alpha-carbon atoms of the FYCO1 LIR domain.

As shown in **Fig. 12**, the residues on the C-terminal of LIR is responsible to form hydrophobic pocket with the LC3. The residues on the N-terminal of LIR interact with the LC3 through hydrophilic bonds. The Leu341 and the aromatic ring of His340 could both have hydrophobic interactions with the aliphatic side chains of Lys65 of LC3. In addition, the oxygen atom on the residue Thr339 contributes to the formation of strong hydrophilic contact with the carbonyl end of the key residue Lys65 (3.7 Å) and Ile66 (4.7 Å). The indole ring of residue Trp338 is inserted into a site surrounded by a conserved group of residues on the LC3, which is a striking feature of the interactions. It plays an important role in forming the hydrophobic interaction in this region with the imidazole ring of His57 (6.5 Å). Another interaction site between the N-terminal portion of LIR and two residues (Leu53 and Pro55) on the surface of the LC3. Ser332, Gly333

and Gly334 are charged. Hydrophilic residues form the salt bridges and hydrogen bonds with the Leu53 and Pro55. We found that Leu53 forms the hydrogen bond with the hydroxyl group of Ser332 (4.5Å), carbonyl group of Ser332 (4.2Å) and the amino group of Gly333 (3.1Å). The nitrogen of the Pro55 acts as a hydrogen bond acceptor and could interact with the amino group of Gly333 (4.4Å), amino group of Gly334 (5.0Å) and the carbonyl group of Gly333 (3.3Å).

To confirm the interacting structure of LC3-LIR, point mutation was inserted into the indicated amino acids of LIR in p62 by replacement with alanine.(90) The formation of LC3-LIR complex was significantly reduced in W338A and L341A mutants. The results suggested that the hydrophobic residues WXXL (338 and 341) are important for protein-protein interactions of LC3.

	Leu53	Pro55	His57	Lys65
Ser332	4.5*			
Gly333	4.2*	3.3*/4.4*		
Trp338			6.5#	
Thr339				3.7*
His340				4.5#
Leu341				3.0#

Table 1. Important residues in LC3-LIR binding.

This table shows all of the distances (~ Å) of interactions between important residues. The first column demonstrates residues on the LIR domain, and the first row demonstrates residues on the LC3. (*) shape represents hydrophilic bonds while (#) shape represents hydrophobic interactions.

3.3 BINDING OF p62 WITH UBIQUITIN

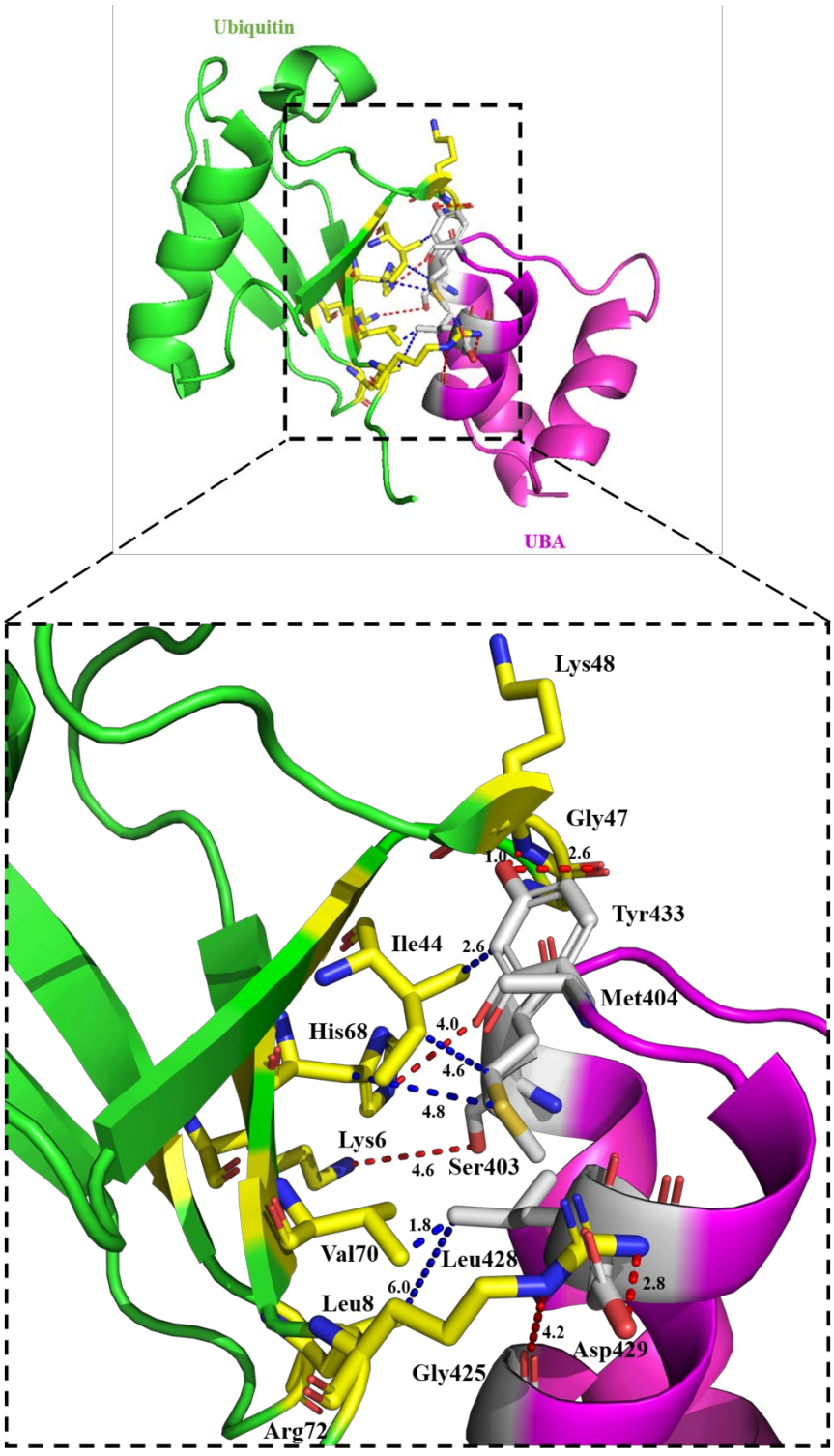

Figure 13. Intermolecular view of p62 binding with ubiquitin through its UBA domain.

The upper one shows the interactions between UBA domain (magentas) of p62 and ubiquitin (green). Red dotted lines represent hydrophilic bonds while the blue one means the hydrophobic interactions. Important residues from the UBA domain was marked as white sticks by elements. Important residues from the ubiquitin are shown as yellow sticks by elements. The length of predicted interaction has been marked. The bottom one is the zoom-in view showing the interactions clearer.

The relative orientations of our p62 LIR domain and LC3 were based on the reported crystal structure of NBR1 (Human Autophagy Receptor) UBA domain bound with ubiquitin. Homo crystal structure of UBA-ubiquitin complex (PDB ID: 2MJ5) has been reported. Superimposition and adjustment were applied to obtain an accurate complex. Briefly, our UBA domain of p62 was superimposed onto the alpha-carbon atoms of the NBR1 UBA domain.

Fig. 13 explains that the ubiquitin intermolecular binding interface of p62 UBA is largely determined by conserved hydrophobic interactions. The cluster of strong hydrophobic bonds are identified between the side chains of Leu8, Ile44, His68, Val70 on ubiquitin and the aliphatic chains of Met404, Leu428, permitting the formation of the large hydrophobic pocket in this region. Specifically, the sulfur atom on methionine can form a hydrophobic bond with the aromatic ring of histidine (4.8 Å). The hydrophobic bond between valine and leucine is the strongest one, only at the distance of 1.8 Å. Polar contacts such as salt bridges and hydrogen bonds are present in the interactions between UBA and ubiquitin as well. Residue Ser403 of the p62 UBA plays an indispensable role on the formation of polar interactions. The hydroxyl group of the residue Ser403 is positioned in close proximity to the side chain amino group of Lys6 at the distance of 4.6 Å,

forming the hydrogen bond. In addition, the carbonyl group at the other end of Ser403 could also form the hydrogen bond with the imidazole ring of His68 on ubiquitin. By contrast, other UBA domains such as NBR1 and HR23A UBA-1 have a glutamine or alanine, respectively, at the equivalent site. Basic amino acids Arg72 of ubiquitin and acidic amino residue Asp429 of UBA should have the electrostatic interaction with each other. Furthermore, we could observe the formation of hydrogen bond between amino groups of Arg72 and hydroxyl group of Asp429 (2.8 Å) or the carbonyl group of Gly425 (4.2 Å). Interestingly, residues on the C-terminal of UBA domain such as Tyr433 can contribute to both the hydrophobic and hydrophilic bonds. The benzene ring of Tyr433 has the hydrophobic interaction with the side chain of Ile44. The hydrogen atom on the hydroxyl group of Tyr433 can form the very strong hydrogen bond with the hydrogen on the amino group of two other amino acids of ubiquitin, Gly47 and Lys48, at the distance of 2.6 Å and 1.0 Å, respectively.

It has been reported that the phosphorylated modification of Ser403 significantly increase the polyubiquitin binding of p62 *in vivo*, enhancing the autophagic clearance of ubiquitinated proteins.(65, 91, 92) M404T / M404V mutants highly destabilized UBA. Their results show that Tyr433 could play a key role not only in the dimerization but also the ubiquitin binding for UBA. Moreover, the dimerization and ubiquitin binding were mutually exclusive, in agreement with the finding of Isogai et al.(65)

	Lys6	Leu8	Ile44	Gly47	Lys48	His68	Val70	Arg72
Ser403	4.6*					4.0*		
Met404			4.6#			4.8#		
Gly425								4.2*
Leu428		6.0#					1.8#	
Asp429								2.8*
Tyr433			2.6#	2.6*	1.0*			

Table 2. Important residues in Ubiquitin-UBA binding.

This table shows all of the distances (~ Å) of interactions between important residues. The first column demonstrates residues on the UBA domain, and the first row demonstrates residues on the ubiquitin. (*) shape represents hydrophilic bonds while (#) shape represents hydrophobic interactions.

3.4 BINDING OF p62 WITH PKCζ

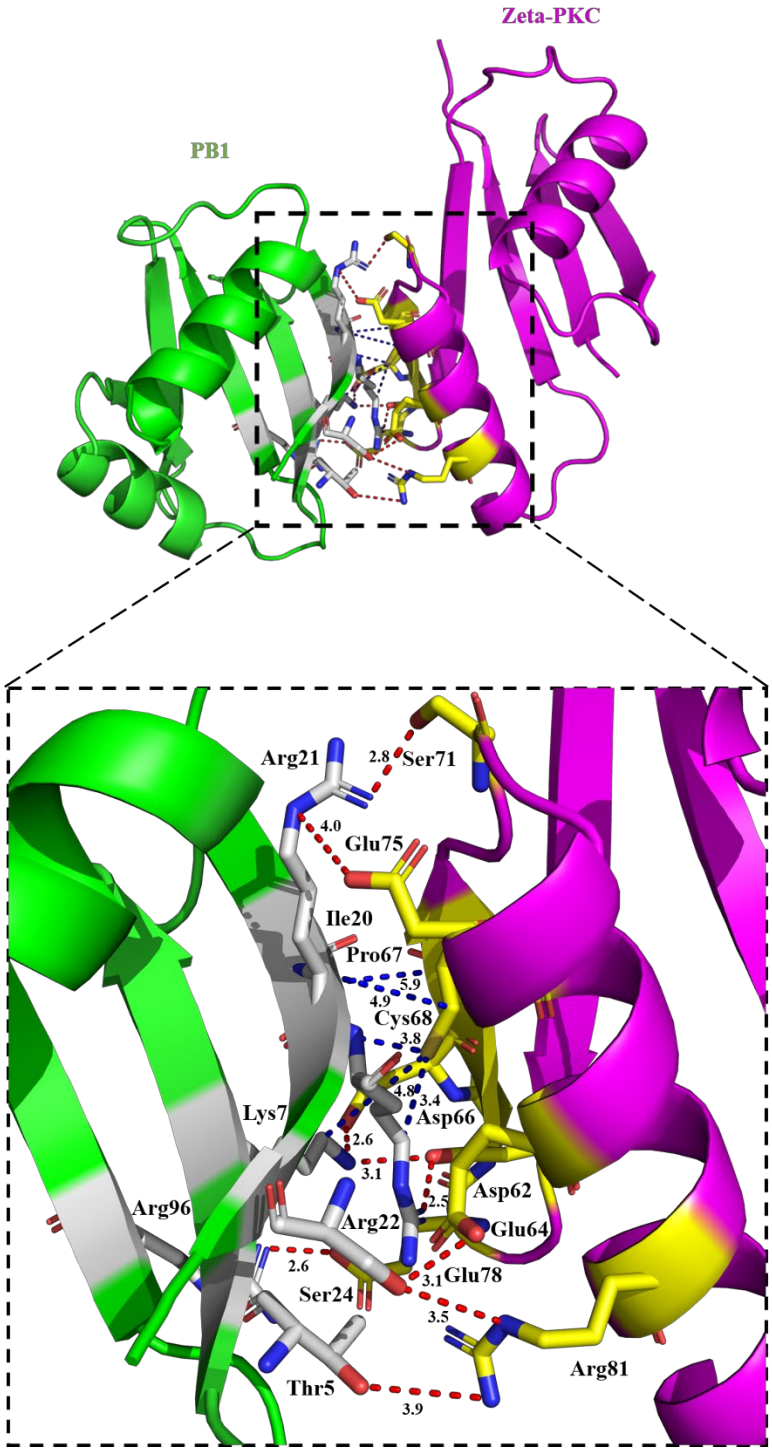

Figure 14. Intermolecular view of p62 binding with PKCζ through its PB1 domain.

The upper one shows the interactions between PB1 domain of p62 (green) and PKCζ (magentas). Red dotted lines represent hydrophilic bonds while the blue one means the hydrophobic interactions. Important residues from the PB1 domain of p62 was marked as white sticks by elements. Important residues form the PB1 domain of PKCζ are shown as yellow sticks by elements. The length of predicted interaction has been marked. The right one is the zoom-in view displaying the interactions clearer.

The protein kinase C (PKC) family comprises three classes: conventional (cPKC: α, β and γ), novel (nPKC: δ, ε, η andθ), and atypical (aPKC: ζ and ι/λ classes). Both PKCζ and p62 are multidomain proteins, each containing a PB1 domain. The PB1 domain is classified into three types, type I, type II, and type I/II.(93) Type I contains a motif of 28 amino acid residues with highly conserved acidic and hydrophobic residues named the OPCA motif. Type II contains a conserved lysine residue on the side opposite to the OPCA motif. Type I/II contains the OPCA motif and the conserved lysine residue, and this can do self-interact in a front-to-back topology. The p62 PB1 contains both the OPCA motif and the conserved lysine residue and is classified into type I/II. p62-PB1 domain provides the basic suface to form heterodimeric complex with the acidic OPCA motif of PKCζ-PB1 through electrostatic interactions. Both of the p62-PB1 and PKCζ-PB1 are composed of five-stranded β-sheet (β1-β5) and two α-helices. But this two are able to interact with each other in the 'front-to-back' manner, ie the 'front' β1-β2 hairpin, the basic surface of PB1, binds with 'back' β3-β4 hairpin, the acidic surface. As no PKCζ-PB1 crystal structure has been reported, so we built the homology model using Protein kinase C zeta type as a template (PDB ID: 4MJS, Resolution: 2.5 Å), with a sequence identity of about 88.51%, using

Swiss-model (https://swissmodel.expasy.org/). Since the crystal structure of homotypic PB1-PB1 complex between PKC zeta and p62 has been reported (PDB ID: 4MJS), we respectively superimoposed our p62 PB1 domain with the crystal structure.

Electrostatic interactions play a dominant role among all the interactions between PKCζ-PB1 and p62-PB1. The interaction pattern resembles 'a three-pin plug'. It exists three indispensable functional clusters of residues on the interactive surfaces of the PKCζ-PB1 and p62-PB1, respectively. These six regions, in total, could interact with each other in a pairwise pairing manner. The first pair happens between three acidic residues on the PKCζ-PB1 (Asp62, Glu64 and Asp66) and three basic residues from strands β1, β2 and β5 on the p62-PB1 (Lys7, Arg22 and Arg96). Specificially, secondary amino group of Arg96 forms hydrogen bond with the oxygen on the carboxyl group of Glu64 at the distance of 2.6 Å. The oxygen on the carboxyl group of Asp62 forms hydrogen bond with Lys7 (3.1 Å) and Arg22 (2.5 Å). The oxygen on the carboxyl group of Asp66 could form the salt bridge with amino group of Lys7 (2.6 Å). Secondly, Arg21 of p62-PB1 could form strong hydrogen bonds with both Ser71 and salt bridge with Glu75 on helix α-2 of PKCζ-PB1, at the distance of 2.8 Å and 4.0 Å, respectively. The third pair forms between residues from p62-PB1 (Thr5 and Ser24) and residues from PKCζ-PB1 (Arg81 and Glu78). Specificially, hydrogxyl group of Ser24 could have hydrogen bonds with both Arg81 (3.5 Å) and Glu78 (3.1 Å). Another hydrogen bond is formed between amino groups of Arg81 and Thr5. These three pairs work together and facilitate the stability of the binding interface between PKCζ-PB1 and p62-PB1. Futhermore, hydrophobic bonds also contribute to the interactive binding between PKCζ-PB1 and p62-PB1. More specifially, it is a binding between aliphatic side chains of Cys68 on the PKCζ-PB1 and residues on the p62-PB1 (Lys7, Arg21, Arg22 and Ile20). Ile 20 could also form hydrogphobic interactions with the the aromatic ring of Pro67 from PKCζ-PB1.

It has been reported that PKCζ mutants (D62A, E64A, D66A and E75A) drastically abrogated the binding to p62-PB1AM.(93) By contrast, mutations of Ser71, Arg81 and Glu78 displayed little effect on the hetero-complex formation. Residue Trp60 within the OPCA motif of PKCζ-PB1 had been shown to mediate the homotypic PB1-PB1 interaction. Although this residue is not directly involved in the PB1 complex formation, it participates in the hydrophobic core formation of the PB1 domain. Pull-down assays have shown that substitutions of the basic residues Lys7, Arg21, Arg22 and Arg96 of p62-PB1 completely ablated the formation of heterocomplex by disrupting the electrostatic interactions, while neither of the mutations at site B3 (T5A and S24A) interfered with its hetero-interaction with PKCζ-PB1. These data demonstrate that the electrostatic interactions at the first and second pairs are the major forces in the formation of a stable complex between PKCζ-PB1 and p62-PB1, while the hydrogen bonds formed in the third pair exert an auxiliary function in specific recognition.

	Asp62	Glu64	Asp66	Pro67	Cys68	Ser71	Glu75	Glu78	Arg81
Thr5									3.9*
Lys7	3.1*		2.4*		4.8#				
Ile20				5.9#	4.9#				
Arg21					3.8#	2.8*	4.0*		
Arg22	2.5*				3.4#				
Ser24								3.1*	3.5*
Arg96		2.6*							

Table 3. Important residues in PKCζ-PB1 binding.

This table shows all of the distances (~ Å) of interactions between important residues. The first column demonstrates residues on the p62-PB1 domain, and the first row demonstrates residues on the PKCζ-PB1. (*) shape represents hydrophilic bonds while (#) shape represents hydrophobic interactions.

3.5 BINDING OF p62 WITH RIP1

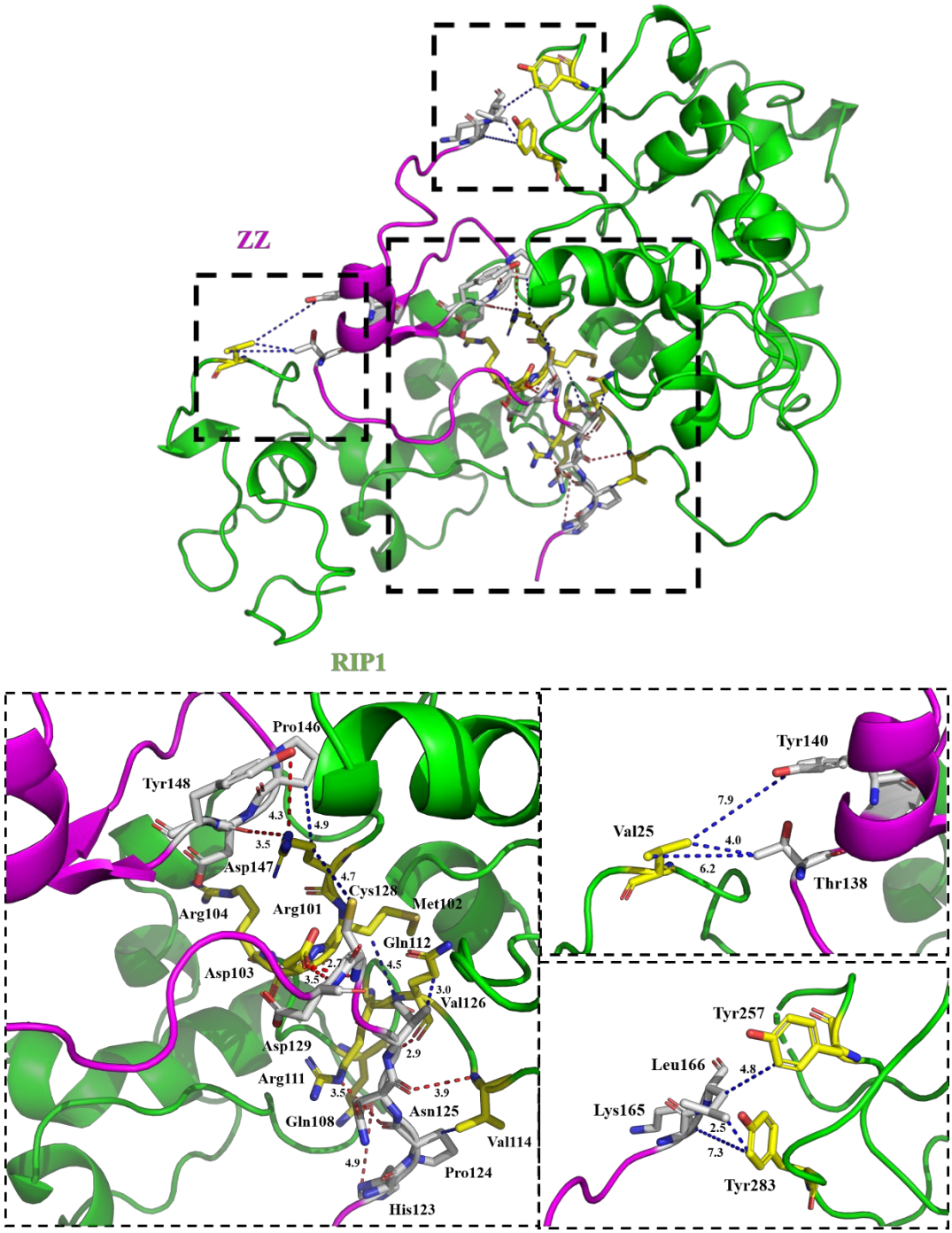

Figure 15. Intermolecular view of p62 binding with RIP1 through its ZZ domain.

The upper one shows the interactions between RIP1 (green) and ZZ domain of p62 (magentas). Red dotted lines represent hydrophilic bonds while the blue one means the hydrophobic

interactions. Important residues from the ZZ domain of p62 was marked as white sticks by elements. Important residues from the RIP1 are shown as yellow sticks by elements. The length of predicted interaction has been marked. The bottom three are the zoom-in views and make the interactions of three sites clearer.

Our results showed that the RIP1 ID (residues from 290 to 582) mainly interacted with ZZ domain. This conformation was supported by the work of Sanz et al. "The death and the kinase domains of RIP1 are dispensable, whereas the intermediary domain is sufficient for the interactions with p62. Also, this correlates with the observation that intermediary domain is sufficient, where the death domain of RIP is dispensable, for NF-κB activation." (94, 95)

In order to explore the molecular interactions between ZZ domain and RIP1, we docked RIP1 (residues from 290 to 582) into our p62 model by using ZDOCK server. ZDOCK was a rigid-body docking program. After finishing the dockings, we compared the docking results and selected the structure with the lowest RMSDs as the best conformation. The docking result of p62-RIP1 complex in each cluster is shown in **Fig. 15**. To further analyze the docking results of p62 and RIP1, we selected ZZ domain (in our p62 model) and LC3 for clarity, as shown in **Fig. 15**.

Fig. 15 have shown three main binding interfaces between p62 ZZ domain and RIP1 in detail. The first binding site described in **Fig. 15** consists of two residues (Tyr257 amd Tyr283) from RIP1 and two residues (Lys165 and Leu166) from ZZ domain. The aliphatic side chain of Leu166 could form the strong hydrophobic interactions with the aromatic ring of Tyr257 (4.8 Å) and Tyr283 (2.5 Å). The other hydrophobic linkage is formed between Tyr283 and Lys165. The

second binding site is similar with the first one, mainly composed of hydrophobic interactions. For example, Val25 could interact with Thr138 and the aromatic ring of Tyr 140 on the ZZ domain at the distance of 4.0 Å and 7.9 Å, respectively. To the contrast, hydrophilic force plays a dominant role in the next binding interface to be mentioned. Arg101 from the RIP1 could form hydrogen bonds with both the Asp147 (3.5 Å) and Tyr148 (4.3 Å). The oxygen atom on the Asp103 of the ZZ could interact with the amino groups of Cys128 (2.7 Å) and Asp129 (3.5 Å) from the RIP1. There also exists a cluster of residues (His123, Pro124) on the ZZ domain, which could form the hydrogen bonds with the hydrophilic cluster of residues (Gln108, Arg111 and Val114) on the RIP1. Futhermore, due to the presence of residues with long aliphatic chain such as Arg101, Met102, Gln112 and Val114 on the RIP1, there are also some hydrophobic linkages between those resides and the other residues on the ZZ domain. For example, the aliphatic chain of Cys128 and Val126 or the aromatic ring of Pro124 and Pro146 on the ZZ domain could participate in forming of those hydrophobic interactions.

	Val25	Arg101	Met102	Gln108	Arg111	Gln112	Val114	Cys128	Asp129	Tyr257	Tyr283
Asp103		3.5*						2.7*	3.5*		
His123				4.9*	3.5*						
Pro124							3.4#				
Asn125							3.9*				
Val126			4.5#			3.0#/2.9*					
Cys128		4.7#									
Thr138	4.0#										
Tyr140	7.9#										
Pro146		4.9#									
Asp147		3.5*									
Tyr148		4.3*									
Lys165											7.3#
Leu166										4.8#	2.5#

Table 4. Important residues in ZZ-RIP1 binding.

This table shows all of the distances (~ Å) of interactions between important residues. The first column demonstrates residues on the ZZ domain, and the first row demonstrates residues on the RIP1. (*) shape represents hydrophilic bonds while (#) shape represents hydrophobic interactions.

3.6 p62 SELF-OLIGOMERIZATION THROUGH PB1 DOMAIN

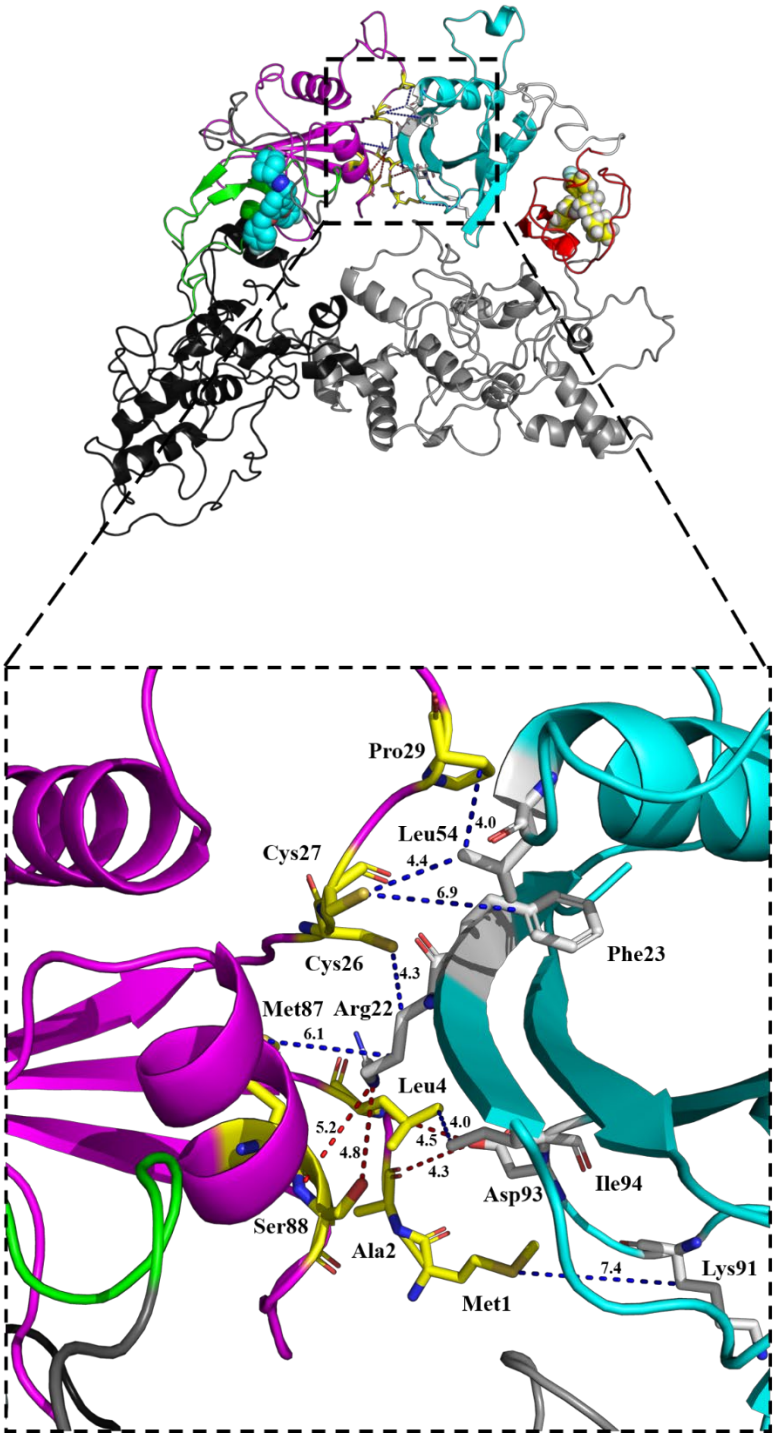

Figure 16. Intermolecular view of p62 self-oligomerization through its PB1 domain (Conf 1). The left one shows the binding conformation of two full-length p62. Hydrophobic bonds are the main forces shown in this **Fig. 16**. XIE2008 binding in the ZZ domain (green and red) is shown as the cyan or yellow spheres. PB1 domains of two p62 are highlighted in magentas and cyan, respectively. Other domains in the two p62s are shown in the gray. Red dotted lines represent hydrophilic bonds while the blue one means the hydrophobic interactions. Important residues from the one of p62 was marked as white sticks by elements. Important residues from the other are shown as yellow sticks by elements. The length of predicted interaction has been marked. Magnified picture in **Fig.16** shows clearer intermolecular interactions of p62 self-oligomerization.

As mentioned above, p62 PB1 domain is classified into TypeI/II so that could self-aggregate through its PB1 domain to be transported to the autophagosome. For the better comprehension of intermolecular interaction of p62 self-oligomerization, we docked two our p62 models with each other by using ZDOCK server. ZDOCK is a rigid-body docking program.

Among the results, 2 possible structures were selected with the lowest RMSDs as the best conformations. Then the models were refined by the molecular simulation (MD). This study generates stable conformation of p62 oligomerized complex, as shown in **Fig. 16**. To further analyze the results, we selected PB1 domain (in our p62 model) for clarity as well.

Fig. 16 has shown the first possible conformation of p62 PB1 domain self-aggregation. The intermolecular interface mainly consists of hydrophobic forces between residues including Met1, Arg22, Phe23, Cys26, Cys27, Pro29, Mer87, Lys91 and Ile94. In detail, the aliphatic chain of Arg 22 from one PB1 domain is able to interact with the sulfur atoms of Cys26 (4.3 Å) and

Met87 (6.1 Å) from the other PB1 domain in a hydrophobic manner. Met1 and Leu4 have hydrophobic bond with Lys91 (7.4 Å) and Ile94 (4.0 Å) through their aliphatic chains, respectively. The aliphatic chain of Leu54 is positioned closely to the aromatic ring of Pro29 and the sulfur atom of Cys27 from the other PB1 domain, which result in the strong hydrophobic interactions in the distance of 4.4 Å and 4.0 Å, respectively. In addition, the sulfur atom of the Cys27 could also be able to form the hydrophobic linkage with the benzene ring of Phe23 (6.9 Å). Even though the hydrophobic force is dominant on the interaction between two PB1 domains, we could also observe four hydrophilic bonds in **Fig. 16**. The carboxyl group of Asp93 form the hydrogen bonds with both the amino group of Leu4 (4.5 Å) and carbonyl group of Ala2 (4.3 Å). Futhermore, the amino group of Arg22 could interact with the Ser88 by forming hydrogen bonds with the hydroxyl group or the amino group of the Ser88.

	Arg22	Phe23	Leu54	Lys91	Asp93	Ile94
Met1				7.4#		
Ala2					4.3*	
Leu4					4.5*	4.0#
Cys26	4.3#					
Cys27		6.9#	4.0#			
Pro29			4.4#			
Met87	6.1#					
Ser88	4.8*/5.2*					

Table 5. Important residues in PB1-PB1 binding.

This table shows all of the distances (~ Å) of interactions between important residues. The first column demonstrates residues on the first PB1 domain, and the first row demonstrates residues

on the second PB1 domain. (*) shape represents hydrophilic bonds while (#) shape represents hydrophobic interactions.

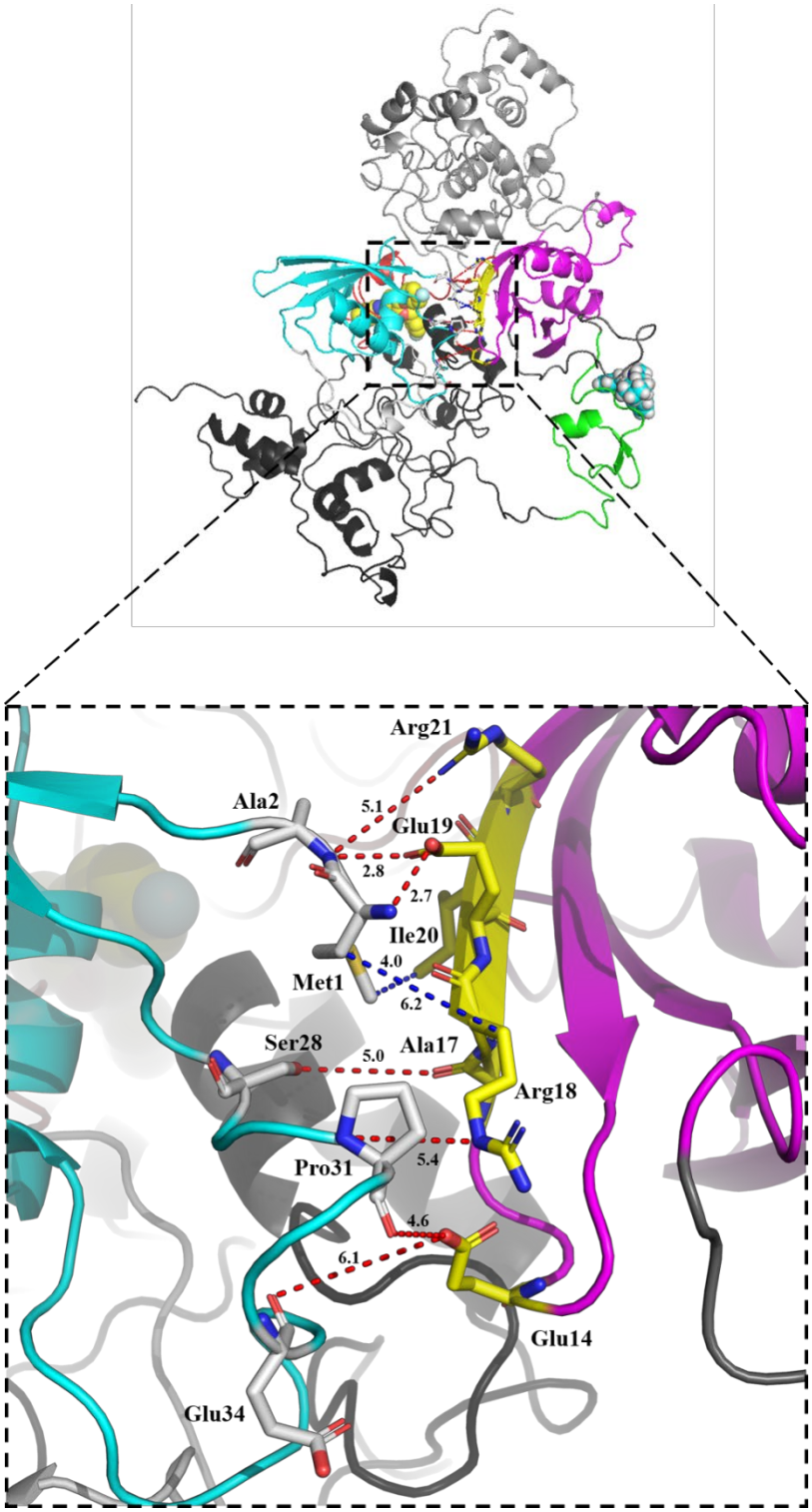

Figure 17. Intermolecular view of p62 self-oligomerization through its PB1 domain (Conf 1). The upper one shows the other binding conformation of two full-length p62s. Hydrophilic bonds are the main forces shown in this **Fig. 17**. Xie2008 bound in the ZZ domain (green and red) was shown as the cyan or yellow spheres. PB1 domains of two p62 are highlighted in magentas and cyan, respectively. Other domains in the two p62s are shown in gray90, gray60, gray40 and gray10 in the pymol. Red dotted lines represent hydrophilic bonds while the blue one means the hydrophobic interactions. Important residues from the one of p62 was marked as white sticks by elements. Important residues from the other are shown as yellow sticks by elements. The length of predicted interaction has been marked. The bottom one is the zoom-in views and make the interactions clearer.

On the contrary, hydrophilic interactions play the leading role in forming PB1-PB1 complex in the second conformation (**Fig. 17**). The important hydrophilic residues include Ala2, Glu14, Ala17, Arg18, Glu19, Arg21, Ser28, Por31 and Glu34. Specifically, the carboxyl group of Glu19 contributes to the formation of salt bridges with amino groups of Met1 (2.7Å) and Ala2 (2.8 Å). In similar, the carboxyl of Glu14 forms the two important hydrogen bonds with Por31 (4.6 Å) and Glu34 (6.1 Å) from the other PB1 domain. Ala2 and Arg21, Ser28 and Ala17, Pro31 and Arg18 could also form the hydrogen bonds with each other in the distance of 5.1 Å, 5.0 Å, 5.4 Å, resulting in the strong hydrophilic interactions between two PB1 domains. Aside from these interactions, the existence of hydrophobic bonds between aliphatic side chains of Met1, Ile20 and Arg18 could not be ignored.

	Glu14	Ala17	Arg18	Glu19	Ile20	Arg21
Met1		6.2#		2.7*	4.0#	
Ala2				2.8*		5.1*
Ser28		5.0*				
Pro31	4.6*		5.4*			
Glu34	6.1*					

Table 6. Important residues in PB1-PB1 binding.

This table shows all of the distances (~ Å) of interactions between important residues. The first column demonstrates residues on the first PB1 domain, and the first row demonstrates residues on the second PB1 domain. (*) shape represents hydrophilic bonds while (#) shape represents hydrophobic interactions.

3.7 DYNAMICAL CROSS-CORRELATIONS BETWEEN p62 PB1 AND ZZ DOMAIN

We performed 100ns MD simulation for p62-p62. Then we obtained the best conformation for the following study. The DynOmics ENM server (http://gnm.csb.pitt.edu/index.php) computes biomolecular systems dynamics for user-uploaded structural coordinates or PDB identifiers, by integrating two widely used elastic network models (ENMs) – the Gaussian Network Model (GNM) and the Anisotropic Network Model (ANM).

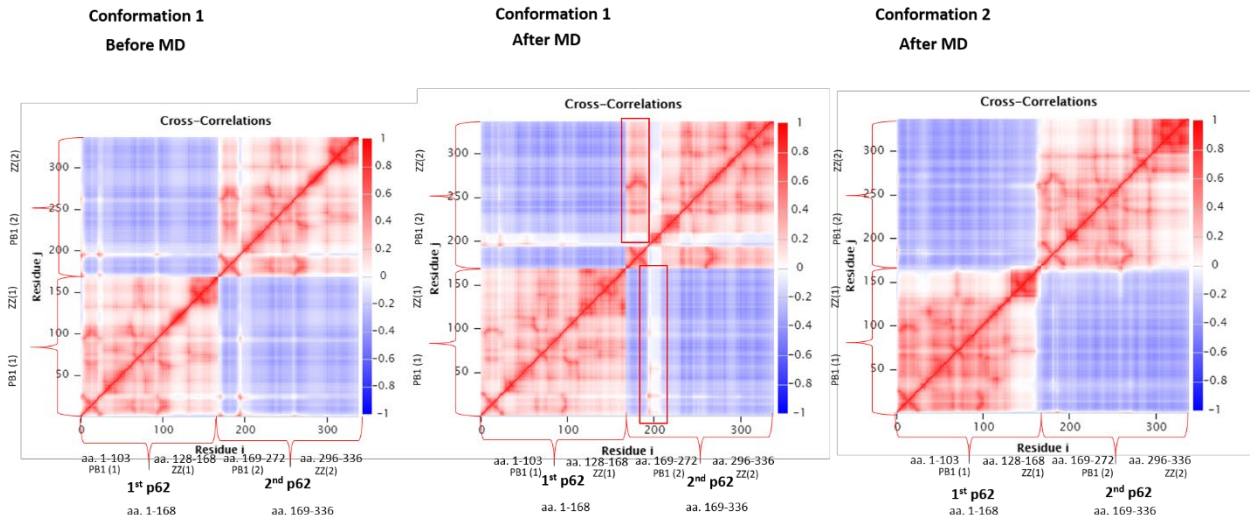

Figure 18. Normalized DCCs obtained by using Gaussian Network Model.

This is a model based on 388 modes at 7.3 Å cutoff radius. Numbers of the nonzero GNM modes that give rise to the best similarity are given in parentheses.

The interactive CC map is restricted to N ≤ 1,000. If N > 500, only 100 nodes will be displayed in both axes by default. Due to the memory limitation, the axes number should ≤ 500. Residue indices along the axes are renumbered for all chains (or molecules/subunits) if the PDB structure has multiple chains, e.g. for two chains A and B, of NA and NB residues, respectively, the first NA entries along either axis refer to chain A, and those in the range (NA+1, NA+NB) refer to chain B.

Our both DCC results validated the importance of residues mentioned above ((Met1, Arg22, Phe23, Cys26, Cys27, Pro29, Mer87, Lys91) and (Ile94, Ala2, Glu14, Ala17, Arg18, Glu19, Arg21, Ser28, Pro31 and Glu34)). In addition, residues 65-72 on the PB1 domain also

shows the relatively high correlations with the residues 139,147,151 on the ZZ domain, which indicates that PB1 could be affected by the fluctuations or conformational changes of ZZ domain. Our compounds like Xie2008 will contribute to the conformational changes of ZZ domain when their binding with each other. Thus, this dynamical Cross-Correlations results reveals that the potential effect of our compound on the p62 PB1-PB1 oligomerization from the computational view.

4.0 CONCLUSION AND DISCUSSION

In this study, firstly, we discussed the relationship among p62, autophagy and diseases. PB1, UBA and LIR of p62 could influence the autophagy process directly, while the other domains like KIR could also affect the other physiological processes like antioxidant response. Signaling pathways mediated by the six domains of p62 will have crosstalk with each other. It is not clear that domains like ZZ would be related to the regulation of autophagy. We looked into the pathogenesis in different autophagy-related diseases including cancer, inflammation and neurodegenerative diseases such as PD, AD, and HD. In general, neurodegenerative diseases could be caused by accumulation of different misfloded protein like α-syn, mHTT and Tau-protein, whose degradation are dependent on the autophagy process. Therefore p62 is the potential therapeautic target for those diseases. However, autophagy as the hall marker of the cancer, the role of it in the cancer are still on debate. Biologists used many methods to inhibit autophagy and observed the outcomes of cancer. These methods includes using 3-methyladenine (3-MA, a PI3K III inhibitor), hydroxychloroquine (HCQ) (lysosomotropic agents that impair fusion between autophagosomes and lysosomes), or knocking down autophagy-related genes, such as ATG5, ATG6 and ATG7.(6) Deletion of Beclin 1 (BECN1, also called ATG6) in mice shows higher incidence of lymphoma, lung cancer and liver cancer. With this respect, the activation of the inducer of the autophagy would be the anti-cancer therapy. But there are also some autophagy inhibitors like β-carotene, lycopene, lutein, quercetin, resveratrol, curcumin and epigallocatechin-3-gallate (EGCG) demonstrating anti-cancer activities in many preclinical and clinical studies.(96, 97) In this way, the inhibition of autophagy could assist cancer therapy.

Then in order to further study on the interactions between p62 domains and their reported partners, we firstly built the full-length p62 using homology model and docked their partners into selected domain of p62. Some non-homo crystal structure of their partners has been reported and we also used the homology model to build the predicted crystal structure of them. We used the Z-DOCK, a rigid protein docking program online and selected the most possible conformation between partners and domains of p62, as shown in the article. The residues on the C-terminal of LIR plays an important role in forming hydrophobic pocket with the LC3. The important residues include Trp338, Thr339, His340 and Leu341 from the LIR and His57 and Lys65 from the LC3. On the other, the N-terminal of LIR is responsible for the formation of hydrophilic interface. The important residues include the Ser332, Gly333, Gly334 from the LIR and Leu53, Pro55 from the LC3. The ubiquitin intermolecular binding interface of p62 UBA is largely determined by conserved hydrophobic interactions. Leu8, Ile44, His68, Val70 on ubiquitin and the aliphatic chains of Met404, Leu428 contribute to the formation of the large hydrophobic pocket in this region. P62-PB1 domain provides the basic suface to form heterodimeric complex with the acidic OPCA motif of PKCζ-PB1 through electrostatic interactions. The binding mode is in front-to-back manner and is like 'three-plugs-in', which means the stable interactions could be contributed by the three different binding sites. RIP1 ID (residues from 290 to 582) mainly interacted with ZZ domain. And there are three main binding interfaces between p62 ZZ domain and RIP1.

Finally, because the p62 PB1 domain is typeI/II, we hypothesized that the self-oligomerization between p62, which is important in autophagy process, could be mediated by the PB1. We used the Z-DOCK program to figure out its possible conformations and predict the important residues involved in the self-ologomerization. In the first possible conformation, the intermolecular interface mainly consist of hydrophobic forces between residues including Met1,

Arg22, Phe23, Cys26, Cys27, Pro29, Mer87, Lys91 and Ile94. On the contrary, hydrophilic interactions play the leading role in forming PB1-PB1 complex in the second conformation. The important hydrophilic residues include Ala2, Glu14, Ala17, Arg18, Glu19, Arg21, Ser28, Por31 and Glu34. Acutually, we found a completely symmetric conformation between those two p62 PB1 domains. However, we observed that this conformation is not stable from the validation of molecular simulation.

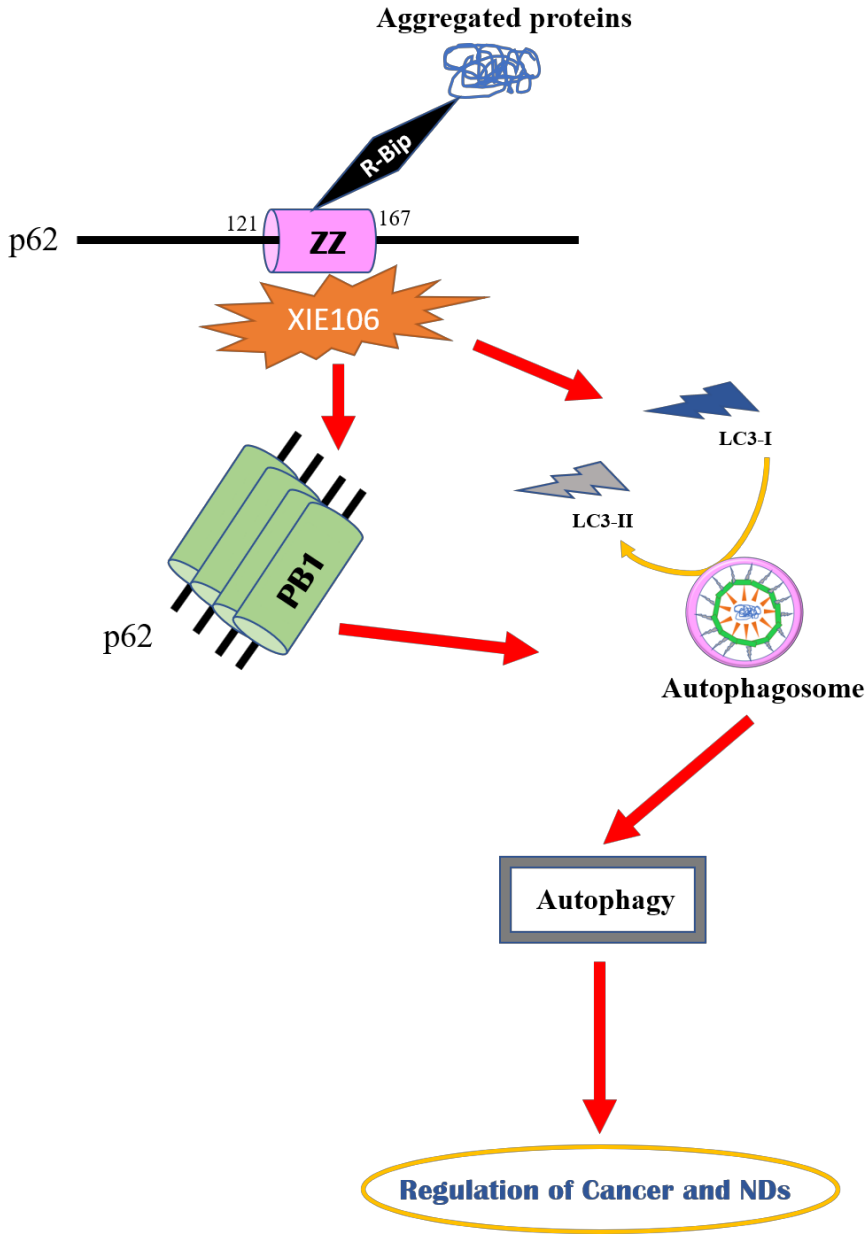

Figure 19. Overview of scheme of this thesis.

Red arrows represent activation of next step. Misfolded protein was linked to the p62 ZZ domain *via* Nt-Arg of R-Bip, then the conformation of p62 would change and enhance the PB1 oligomerization and autophagosome formation. In this way, autophagy could be induced. Our synthesized small molecule like XIE106 plays an important role in this pathway.

5.0 FUTURE PROSPECTIVE

In the current study, all the research are based on the computatinal validation and prediction. There are some known reported experimental data showing the binding between selected domains (ZZ, PB1, LIR, UBA) and their partners. We plan to do biological experiments like point mutation to see if the predicted residues (conformation1: Met1, Arg22, Phe23, Cys26, Cys27, Pro29, Mer87, Lys91 and Ile94; confromation2: Ala2, Glu14, Ala17, Arg18, Glu19, Arg21, Ser28, Por31 and Glu34) would really play an important role in self-oligomerization between p62-PB1 domains. And we also plan to design compounds which could regulate autophagy through binding with p62 specific domain like ZZ and PB1. We hypothesized that one compound could interrupt the self-oligomerization of p62 by showing a good affinity to PB1 domain, which could induce the autophagy and shows its potential therapeutic effect on the neurodegradative diseases like Alzheimer's diseases.

6.0 APPENDIX & ABBRETHROUGHTIONS

AD	Alzheimer's disease
ATG	Autophagy related genes
AMPK	AMP-activated protein kinase
ANM	Anisotropic Network Model
Akt	Protein kinase B
Bip	Binding immunoglobulin protein (BiP)
CK2	Casein kinase 2
ENM	Elastic network models
ER	Endoplasmic reticulum
ERK	Extracellular signal–regulated kinases
FKBP1A	FK506-binding protein 1A
GNM	Gaussian Network Model
HD	Huntington's disease
IL-1	Interleukin 1
KIR	Keap1-interacting region domain
LIR	LC3-interacting region domain

MM/PBSA	Molecular Mechanics/ Poisson–Boltzmann Surface Area
mTORC	Mammalian target of rapamycin complex 1
MAPK	Mitogen-activated protein kinase
MEKK3	Mitogen-activated protein kinase kinase kinase 3
Mhtt	Mutant huntingtin
NRF2	Nuclear factor-like 2
NGF	Nerve growth factor
PE	Phosphatidylethanolamine
PB1	N-terminal Phox1 and Bem1p domain
PI3K	Phosphatidylinositol-3-Kinase
PD	Parkinson's disease
PKC	Protein kinase C
PINK1	PTEN-induced kinase 1
RANKL	RANK ligand
RIP1	Receptor-interacting serine/threonine-protein kinase 1
SFXC	Surflex-Dock GeomX
TB	TRAF6-binding domain

ULK1	Serine/threonine-protein kinase
UPS	Ubiquitin-Proteasome System
UBA	Ubiquitin-associated domain
ZZ	Zinc finger domain
α-syn	α-synuclein

7.0 BIBLIOGRAPHY

1. Levine B. Eating oneself and uninvited guests: autophagy-related pathways in cellular defense. Cell. 2005;120(2):159-62.
2. You L, Jin S, Zhu L, Qian W. Autophagy, autophagy-associated adaptive immune responses and its role in hematologic malignancies. Oncotarget. 2017;8(7):12374.
3. Shibutani ST, Saitoh T, Nowag H, Münz C, Yoshimori T. Autophagy and autophagy-related proteins in the immune system. Nature Immunology. 2015;16(10):1014.
4. Kroemer G, Mariño G, Levine B. Autophagy and the integrated stress response. Molecular cell. 2010;40(2):280-93.
5. Yang S, Wang X, Contino G, Liesa M, Sahin E, Ying H, Bause A, Li Y, Stommel JM, Dell'Antonio G. Pancreatic cancers require autophagy for tumor growth. Genes & development. 2011.
6. Yang ZJ, Chee CE, Huang S, Sinicrope FA. The role of autophagy in cancer: therapeutic implications. Molecular cancer therapeutics. 2011;10(9):1533-41.
7. Cheng J, Giguère PM, Onajole OK, Lv W, Gaisin A, Gunosewoyo H, Schmerberg CM, Pogorelov VM, Rodriguiz RM, Vistoli G. Optimization of 2-phenylcyclopropylmethylamines as selective serotonin 2C receptor agonists and their evaluation as potential antipsychotic agents. Journal of medicinal chemistry. 2015;58(4):1992-2002.
8. Chen N, Debnath J. Autophagy and tumorigenesis. FEBS letters. 2010;584(7):1427-35.

9. Joung I, Strominger JL, Shin J. Molecular cloning of a phosphotyrosine-independent ligand of the p56lck SH2 domain. Proceedings of the National Academy of Sciences. 1996;93(12):5991-5.

10. Bjørkøy G, Lamark T, Brech A, Outzen H, Perander M, Øvervatn A, Stenmark H, Johansen T. p62/SQSTM1 forms protein aggregates degraded by autophagy and has a protective effect on huntingtin-induced cell death. The Journal of cell biology. 2005;171(4):603-14.

11. Ichimura Y, Kumanomidou T, Sou Y-s, Mizushima T, Ezaki J, Ueno T, Kominami E, Yamane T, Tanaka K, Komatsu M. Structural basis for sorting mechanism of p62 in selective autophagy. Journal of Biological Chemistry. 2008;283(33):22847-57.

12. Liu H, Dai C, Fan Y, Guo B, Ren K, Sun T, Wang W. From autophagy to mitophagy: the roles of P62 in neurodegenerative diseases. Journal of bioenergetics and biomembranes. 2017;49(5):413-22.

13. Lippai M, Lőw P. The role of the selective adaptor p62 and ubiquitin-like proteins in autophagy. BioMed research international. 2014;2014.

14. Korolchuk VI, Mansilla A, Menzies FM, Rubinsztein DC. Autophagy inhibition compromises degradation of ubiquitin-proteasome pathway substrates. Molecular cell. 2009;33(4):517-27.

15. Kirkin V, McEwan DG, Novak I, Dikic I. A role for ubiquitin in selective autophagy. Molecular cell. 2009;34(3):259-69.

16. Nedelsky NB, Todd PK, Taylor JP. Autophagy and the ubiquitin-proteasome system: collaborators in neuroprotection. Biochimica et Biophysica Acta (BBA)-Molecular Basis of Disease. 2008;1782(12):691-9.

17. Cha-Molstad H, Yu JE, Feng Z, Lee SH, Kim JG, Yang P, Han B, Sung KW, Yoo YD, Hwang J, McGuire T, Shim SM, Song HD, Ganipisetti S, Wang N, Jang JM, Lee MJ, Kim SJ, Lee KH, Hong JT, Ciechanover A, Mook-Jung I, Kim KP, Xie X-Q, Kwon YT, Kim BY. p62/SQSTM1/Sequestosome-1 is an N-recognin of the N-end rule pathway which modulates autophagosome biogenesis. Nature Communications. 2017;8(1):102. doi: 10.1038/s41467-017-00085-7.

18. Kirkin V, Lamark T, Sou Y-S, Bjørkøy G, Nunn JL, Bruun J-A, Shvets E, McEwan DG, Clausen TH, Wild P. A role for NBR1 in autophagosomal degradation of ubiquitinated substrates. Molecular cell. 2009;33(4):505-16.

19. Puissant A, Fenouille N, Auberger P. When autophagy meets cancer through p62/SQSTM1. American journal of cancer research. 2012;2(4):397.
20. Shintani T, Huang W-P, Stromhaug PE, Klionsky DJ. Mechanism of cargo selection in the cytoplasm to vacuole targeting pathway. Developmental cell. 2002;3(6):825-37.
21. Rubinsztein DC, Shpilka T, Elazar Z. Mechanisms of autophagosome biogenesis. Current Biology. 2012;22(1):R29-R34.
22. Sou Y-s, Waguri S, Iwata J-i, Ueno T, Fujimura T, Hara T, Sawada N, Yamada A, Mizushima N, Uchiyama Y. The Atg8 conjugation system is indispensable for proper development of autophagic isolation membranes in mice. Molecular biology of the cell. 2008;19(11):4762-75.
23. Johansen T, Lamark T. Selective autophagy mediated by autophagic adapter proteins. autophagy. 2011;7(3):279-96.
24. Law KB, Kim PK. Autophagy: Chapter 5. Ubiquitin and p62 in Selective Autophagy in Mammalian Cells: Elsevier Inc. Chapters; 2013.
25. Moscat J, Diaz-Meco MT. p62 at the crossroads of autophagy, apoptosis, and cancer. Cell. 2009;137(6):1001-4.
26. Katsuragi Y, Ichimura Y, Komatsu M. p62/SQSTM 1 functions as a signaling hub and an autophagy adaptor. The FEBS journal. 2015;282(24):4672-8.
27. Moscat J, Diaz-Meco MT, Albert A, Campuzano S. Cell signaling and function organized by PB1 domain interactions. Molecular cell. 2006;23(5):631-40.
28. Moscat J, Karin M, Diaz-Meco MT. p62 in cancer: signaling adaptor beyond autophagy. Cell. 2016;167(3):606-9.
29. Nakamura K, Kimple AJ, Siderovski DP, Johnson GL. PB1 domain interaction of p62/sequestosome 1 and MEKK3 regulates NF-κB activation. Journal of Biological Chemistry. 2010;285(3):2077-89.
30. Park MH, Hong JT. Roles of NF-κB in cancer and inflammatory diseases and their therapeutic approaches. Cells. 2016;5(2):15.
31. Vandenabeele P, Declercq W, Van Herreweghe F, Berghe TV. The role of the kinases RIP1 and RIP3 in TNF-induced necrosis. Sci Signal. 2010;3(115):re4-re.
32. . H-MSaPVbxpiiI. Necrotic Cell Death. Cell Death in Biology and Diseases. . Yin X-M, Dong Z, editors: Springer (Humana Press); 2014. 397 p.

33. Karch J. Necrotic Cell Death edited by Han-Ming Shen and Peter Vandenabeele. The Quarterly Review of Biology. 2016;91(1):95-. doi: 10.1086/685347.

34. Kendellen MF, Bradford JW, Lawrence CL, Clark KS, Baldwin AS. Canonical and non-canonical NF-κB signaling promotes breast cancer tumor-initiating cells. Oncogene. 2014;33(10):1297-305.

35. Zhou W, Yuan J, editors. Necroptosis in health and diseases. Seminars in cell & developmental biology; 2014: Elsevier.

36. Chen BB, Coon TA, Glasser JR, McVerry BJ, Zhao J, Zhao Y, Zou C, Ellis B, Sciurba FC, Zhang Y. A combinatorial F box protein directed pathway controls TRAF adaptor stability to regulate inflammation. Nature immunology. 2013;14(5):470-9.

37. Teramachi J, Silbermann R, Yang P, Zhao W, Mohammad KS, Guo J, Anderson JL, Zhou D, Feng R, Myint K-Z. Blocking the ZZ domain of sequestosome1/p62 suppresses myeloma growth and osteoclast formation in vitro and induces dramatic bone formation in myeloma-bearing bones in vivo. Leukemia. 2016;30(2):390-8.

38. Lee JW, Park S, Takahashi Y, Wang H-G. The association of AMPK with ULK1 regulates autophagy. PloS one. 2010;5(11):e15394.

39. Dazert E, Hall MN. mTOR signaling in disease. Current opinion in cell biology. 2011;23(6):744-55.

40. Wullschleger S, Loewith R, Hall MN. TOR signaling in growth and metabolism. Cell. 2006;124(3):471-84.

41. Pankiv S, Clausen TH, Lamark T, Brech A, Bruun J-A, Outzen H, Øvervatn A, Bjørkøy G, Johansen T. p62/SQSTM1 binds directly to Atg8/LC3 to facilitate degradation of ubiquitinated protein aggregates by autophagy. Journal of biological chemistry. 2007.

42. Lin X, Li S, Zhao Y, Ma X, Zhang K, He X, Wang Z. Interaction domains of p62: a bridge between p62 and selective autophagy. DNA and cell biology. 2013;32(5):220-7.

43. Komatsu M, Kurokawa H, Waguri S, Taguchi K, Kobayashi A, Ichimura Y, Sou Y-S, Ueno I, Sakamoto A, Tong KI. The selective autophagy substrate p62 activates the stress responsive transcription factor Nrf2 through inactivation of Keap1. Nature cell biology. 2010;12(3):213.

44. Auluck PK, Caraveo G, Lindquist S. α-Synuclein: membrane interactions and toxicity in Parkinson's disease. Annual review of cell and developmental biology. 2010;26:211-33.

45. Jiang P, Mizushima N. Autophagy and human diseases. Cell research. 2014;24(1):69.

46. Choi AM, Ryter SW, Levine B. Autophagy in human health and disease. New England Journal of Medicine. 2013;368(7):651-62.

47. Narendra D, Kane LA, Hauser DN, Fearnley IM, Youle RJ. p62/SQSTM1 is required for Parkin-induced mitochondrial clustering but not mitophagy; VDAC1 is dispensable for both. Autophagy. 2010;6(8):1090-106. doi: 10.4161/auto.6.8.13426.

48. Geisler S, Holmstrom KM, Skujat D, Fiesel FC, Rothfuss OC, Kahle PJ, Springer W. PINK1/Parkin-mediated mitophagy is dependent on VDAC1 and p62/SQSTM1. Nat Cell Biol. 2010;12(2):119-31. doi: http://www.nature.com/ncb/journal/v12/n2/suppinfo/ncb2012_S1.html.

49. Moors TE, Hoozemans JJ, Ingrassia A, Beccari T, Parnetti L, Chartier-Harlin M-C, van de Berg WD. Therapeutic potential of autophagy-enhancing agents in Parkinson's disease. Molecular neurodegeneration. 2017;12(1):11.

50. Ahmed Z, Tabrizi S, Li A, Houlden H, Sailer A, Lees A, Revesz T, Holton J. A Huntington's disease phenocopy characterized by pallido-nigro-luysian degeneration with brain iron accumulation and p62-positive glial inclusions. Neuropathology and applied neurobiology. 2010;36(6):551-7.

51. Rué L, López-Soop G, Gelpi E, Martínez-Vicente M, Alberch J, Pérez-Navarro E. Brain region-and age-dependent dysregulation of p62 and NBR1 in a mouse model of Huntington's disease. Neurobiology of disease. 2013;52:219-28.

52. Ma S, Attarwala I, Xie X-Q. SQSTM1/p62: a potential target for neurodegenerative disease. ACS chemical neuroscience. 2019.

53. Metzger S, Saukko M, Van Che H, Tong L, Puder Y, Riess O, Nguyen HP. Age at onset in Huntington's disease is modified by the autophagy pathway: implication of the V471A polymorphism in Atg7. Human genetics. 2010;128(4):453-9.

54. Martin DD, Ladha S, Ehrnhoefer DE, Hayden MR. Autophagy in Huntington disease and huntingtin in autophagy. Trends in neurosciences. 2015;38(1):26-35.

55. Metzger S, Walter C, Riess O, Roos RA, Nielsen JE, Craufurd D, Nguyen HP, Network RIotEHsD. The V471A polymorphism in autophagy-related gene ATG7 modifies age at onset specifically in Italian Huntington disease patients. PLoS One. 2013;8(7):e68951.

56. Verri M, Pastoris O, Dossena M, Aquilani R, Guerriero F, Cuzzoni G, Venturini L, Ricevuti G, Bongiorno A. Mitochondrial alterations, oxidative stress and neuroinflammation in Alzheimer's disease. SAGE Publications Sage UK: London, England; 2012.
57. Hanger DP, Anderton BH, Noble W. Tau phosphorylation: the therapeutic challenge for neurodegenerative disease. Trends in molecular medicine. 2009;15(3):112-9.
58. Du Y, Wooten MC, Gearing M, Wooten MW. Age-associated oxidative damage to the p62 promoter: implications for Alzheimer disease. Free Radical Biology and Medicine. 2009;46(4):492-501.
59. Kobayashi M, Yamamoto M. Molecular mechanisms activating the Nrf2-Keap1 pathway of antioxidant gene regulation. Antioxidants & redox signaling. 2005;7(3-4):385-94.
60. Luo Y, Bolon B, Kahn S, Bennett BD, Babu-Khan S, Denis P, Fan W, Kha H, Zhang J, Gong Y. Mice deficient in BACE1, the Alzheimer's β-secretase, have normal phenotype and abolished β-amyloid generation. Nature neuroscience. 2001;4(3):231.
61. Sennvik K, Fastbom J, Blomberg M, Wahlund L-O, Winblad B, Benedikz E. Levels of α- and β-secretase cleaved amyloid precursor protein in the cerebrospinal fluid of Alzheimer's disease patients. Neuroscience letters. 2000;278(3):169-72.
62. Saio T, Yokochi M, Inagaki F. The NMR structure of the p62 PB1 domain, a key protein in autophagy and NF-κB signaling pathway. J Biomol NMR. 2009;45(3):335-41.
63. Ichimura Y, Kumanomidou T, Sou Y-s, Mizushima T, Ezaki J, Ueno T, Kominami E, Yamane T, Tanaka K, Komatsu M. Structural basis for sorting mechanism of p62 in selective autophagy. J Biol Chem. 2008;283(33):22847-57.
64. Komatsu M, Kurokawa H, Waguri S, Taguchi K, Kobayashi A, Ichimura Y, Sou Y-S, Ueno I, Sakamoto A, Tong KI. The selective autophagy substrate p62 activates the stress responsive transcription factor Nrf2 through inactivation of Keap1. Nature Cell Biol. 2010;12(3):213-23.
65. Isogai S, Morimoto D, Arita K, Unzai S, Tenno T, Hasegawa J, Sou Y-s, Komatsu M, Tanaka K, Shirakawa M. Crystal structure of the ubiquitin-associated (UBA) domain of p62 and its interaction with ubiquitin. J Biol Chem. 2011;286(36):31864-74.
66. SYBYL-X 1.3, Tripos International, 1699 South Hanley Rd., St. Louis, Missouri, 63144, USA,2010.

67. Cha-Molstad H, Yu JE, Feng Z, Lee SH, Kim JG, Yang P, Han B, Sung KW, Yoo YD, Hwang J. p62/SQSTM1/Sequestosome-1 is an N-recognin of the N-end rule pathway which modulates autophagosome biogenesis. Nature communications. 2017;8(1):102.

68. Schwede T, Kopp J, Guex N, Peitsch MC. SWISS-MODEL: an automated protein homology-modeling server. Nucleic acids research. 2003;31(13):3381-5.

69. Jain AN. Scoring noncovalent protein-ligand interactions: a continuous differentiable function tuned to compute binding affinities. J Comput Aided-Mol Des. 1996;10(5):427-40.

70. Chen J-Z, Wang J, Xie X-Q. GPCR structure-based virtual screening approach for CB2 antagonist search. J Chem Inf Model. 2007;47(4):1626-37.

71. Kozakov D, Hall DR, Beglov D, Brenke R, Comeau SR, Shen Y, Li K, Zheng J, Vakili P, Paschalidis IC. Achieving reliability and high accuracy in automated protein docking: ClusPro, PIPER, SDU, and stability analysis in CAPRI rounds 13–19. Proteins: Structure, Function, and Bioinformatics. 2010;78(15):3124-30.

72. Tovchigrechko A, Vakser IA. GRAMM-X public web server for protein–protein docking. Nucleic Acids Res. 2006;34(suppl 2):W310-W4.

73. Pierce BG, Hourai Y, Weng Z. Accelerating protein docking in ZDOCK using an advanced 3D convolution library. PloS One. 2011;6(9):e24657.

74. Maier JA, Martinez C, Kasavajhala K, Wickstrom L, Hauser KE, Simmerling C. ff14SB: improving the accuracy of protein side chain and backbone parameters from ff99SB. Journal of chemical theory and computation. 2015;11(8):3696-713.

75. Dickson CJ, Madej BD, Skjevik ÅA, Betz RM, Teigen K, Gould IR, Walker RC. Lipid14: the amber lipid force field. Journal of chemical theory and computation. 2014;10(2):865-79.

76. Jorgensen WL, Chandrasekhar J, Madura JD, Impey RW, Klein ML. Comparison of simple potential functions for simulating liquid water. The Journal of chemical physics. 1983;79(2):926-35.

77. Jakalian A, Jack DB, Bayly CI. Fast, efficient generation of high-quality atomic charges. AM1-BCC model: II. Parameterization and validation. Journal of computational chemistry. 2002;23(16):1623-41.

78. Wang J, Wolf RM, Caldwell JW, Kollman PA, Case DA. Development and testing of a general amber force field. Journal of computational chemistry. 2004;25(9):1157-74.

79. Wang J, Wang W, Kollman PA, Case DA. Automatic atom type and bond type perception in molecular mechanical calculations. Journal of molecular graphics and modelling. 2006;25(2):247-60.
80. Götz AW, Williamson MJ, Xu D, Poole D, Le Grand S, Walker RC. Routine microsecond molecular dynamics simulations with AMBER on GPUs. 1. Generalized born. Journal of chemical theory and computation. 2012;8(5):1542-55.
81. Salomon-Ferrer R, Götz AW, Poole D, Le Grand S, Walker RC. Routine microsecond molecular dynamics simulations with AMBER on GPUs. 2. Explicit solvent particle mesh Ewald. Journal of chemical theory and computation. 2013;9(9):3878-88.
82. Case D, Cerutti D, Cheatham T, Darden T, Duke R, Giese T, Gohlke H, Goetz A, Greene D, Homeyer N. AMBER 2016, University of California. San Francisco; 2016.
83. Loncharich RJ, Brooks BR, Pastor RW. Langevin dynamics of peptides: The frictional dependence of isomerization rates of N-acetylalanyl-N′-methylamide. Biopolymers. 1992;32(5):523-35.
84. Izaguirre JA, Catarello DP, Wozniak JM, Skeel RD. Langevin stabilization of molecular dynamics. The Journal of chemical physics. 2001;114(5):2090-8.
85. Darden T, York D, Pedersen L. Particle mesh Ewald: An N· log (N) method for Ewald sums in large systems. The Journal of chemical physics. 1993;98(12):10089-92.
86. Essmann U, Perera L, Berkowitz ML, Darden T, Lee H, Pedersen LG. A smooth particle mesh Ewald method. The Journal of chemical physics. 1995;103(19):8577-93.
87. Ryckaert J-P, Ciccotti G, Berendsen HJ. Numerical integration of the cartesian equations of motion of a system with constraints: molecular dynamics of n-alkanes. Journal of Computational Physics. 1977;23(3):327-41.
88. Wang J, Hou T. Develop and test a solvent accessible surface area-based model in conformational entropy calculations. Journal of chemical information and modeling. 2012;52(5):1199-212.
89. Hawkins GD, Cramer CJ, Truhlar DG. Parametrized models of aqueous free energies of solvation based on pairwise descreening of solute atomic charges from a dielectric medium. The Journal of Physical Chemistry. 1996;100(51):19824-39.
90. Olsvik HL, Lamark T, Takagi K, Larsen KB, Evjen G, Øvervatn A, Mizushima T, Johansen T. FYCO1 contains a C-terminally extended, LC3A/B-preferring LC3-interacting region (LIR)

motif required for efficient maturation of autophagosomes during basal autophagy. Journal of Biological Chemistry. 2015;290(49):29361-74.

91. Walinda E, Morimoto D, Sugase K, Konuma T, Tochio H, Shirakawa M. Solution structure of the ubiquitin-associated (UBA) domain of human autophagy receptor NBR1 and its interaction with ubiquitin and polyubiquitin. Journal of Biological Chemistry. 2014;289(20):13890-902.

92. Isogai S, Morimoto D, Arita K, Unzai S, Tenno T, Hasegawa J, Sou Y-s, Komatsu M, Tanaka K, Shirakawa M. Crystal structure of the ubiquitin-associated (UBA) domain of p62 and its interaction with ubiquitin. Journal of Biological Chemistry. 2011;286(36):31864-74.

93. Ren J, Wang J, Wang Z, Wu J. Structural and biochemical insights into the homotypic PB1-PB1 complex between PKCζ and p62. Science China Life Sciences. 2014;57(1):69-80.

94. Sanz L, Sanchez P, Lallena MJ, Diaz-Meco MT, Moscat J. The interaction of p62 with RIP links the atypical PKCs to NF-κB activation. The EMBO journal. 1999;18(11):3044-53.

95. Hsu H, Huang J, Shu H-B, Baichwal V, Goeddel DV. TNF-dependent recruitment of the protein kinase RIP to the TNF receptor-1 signaling complex. Immunity. 1996;4(4):387-96.

96. Choi KS. Autophagy and cancer. Experimental & molecular medicine. 2012;44(2):109.

97. Zhao Y, Hu X, Zuo X, Wang M. Chemopreventive effects of some popular phytochemicals on human colon cancer: A review. Food & function. 2018;9(9):4548-68.